DESIGN AND ANALYSIS OF A MILLIMETER WAVE FULL-DUPLEX ANTENNA

M.Tech. Thesis

By

KUMARI KAMINI

DEPARTMENT OF ELECTRICAL ENGINEERING
INDIAN INSTITUTE OF TECHNOLOGY INDORE

JUNE 2023

DESIGN AND ANALYSIS OF A MILLIMETER WAVE FULL-DUPLEX ANTENNA

A THESIS

Submitted in partial fulfillment of the requirements for the award of the degree
of
Master of Technology

by
KUMARI KAMINI

DEPARTMENT OF ELECTRICAL ENGINEERING
INDIAN INSTITUTE OF TECHNOLOGY INDORE
JUNE 2023

INDIAN INSTITUTE OF TECHNOLOGY INDORE

CANDIDATE'S DECLARATION

I hereby certify that the work which is being presented in the thesis entitled **DESIGN AND ANALYSIS OF A MILLIMETER WAVE FULL-DUPLEX ANTENNA** in the partial fulfillment of the requirements for the award of the degree of **MASTER OF TECHNOLOGY** and submitted in the **DEPARTMENT OF ELECTRICAL ENGINEERING, Indian Institute of Technology Indore**, is an authentic record of my own work carried out during the time period from August 2021 to June 2023 under the supervision of Dr. Saptarshi Ghosh, Assistant Professor, IIT Indore.

The matter presented in this thesis has not been submitted by me for the award of any other degree of this or any other institute.

Kumari Kamini

07-06-2023

KUMARI KAMINI

This is to certify that the above statement made by the candidate is correct to the best of my/our knowledge.

Saptarshi Ghosh

Dr. Saptarshi Ghosh
(Thesis supervisor)

Kumari Kamini has successfully given his/her M.Tech. Oral Examination held on **12th May, 2023**.

Saptarshi Ghosh

Signature of Supervisor of M.Tech. thesis
Date: 11-06-23

Convener, DPGC
Date: 11-06-23

Vijay AS

Signature of PSPC Member#1
Date: 11-06-23

Ayan Mondal

Signature of PSPC Member#2
Date: 11-06-23

ACKNOWLEDGEMENTS

I would like to acknowledge and pay my warmest regard to my mentor, Dr. Saptarshi Ghosh Sir because the work presented in this thesis is by far the most significant achievement in my life, and it would have been inconceivable without his constant support and encouragement. I am truly grateful to him for his invaluable guidance and mentorship throughout this process.

I would also like to thank all the PSPC members Assistant Prof. Dr. Vijay A.S and Assistant Prof. Dr. Ayan Mondal for their questions and suggestions which have motivated me to work more diligently towards my research work. I would like to thank IIT Indore for all the facilities and Ministry of Education for financial support.

A special gratitude to my senior Post doc. Fellow, Dr. Mohammad Ameen for expert guidance and for sharing practical knowledge with me and senior Ph.D. Scholar, Maharana Pratap Singh for giving full effort in sharing technical concepts and clearing doubts related to this project work with me and Ph.D. Scholar, Akhil Gouda for helping me in writing this thesis and sharing HFSS knowledge. I also want to thank my lab-mate Praneet Jain for their help, cooperation, and encouragement.

Finally, my heartfelt gratitude towards my family for their tireless love and support and their unceasing encouragement and moral support throughout this journey. I would like to thank all my friends who made my journey at IIT Indore an indelible and gratifying experience.

Kumari Kamini

Abstract

As wireless technologies continue to evolve, we all want faster internet and more data on our devices. The current 4G networks were created to meet these demands, but they are no longer enough to handle the increasing number of users and their need for faster speeds. That is why we are transitioning to a new type of wireless communication called 5G, which will use a higher frequency called millimeter-wave (mm-wave) spectrum. This will help us achieve even faster internet access and support the growing number of devices that need to connect to the network. To fulfill the demanding data rate and better utilization of the frequency bands full-duplex is one of the growing techniques. In the conventional communication system, either signal can be transmitted or received on the same channel, whereas in an in-band full-duplex (IBFD) antenna, transmitting and receiving of the signal take place simultaneously at a single frequency. The objective of this thesis is to design and analyze millimeter wave full-duplex antenna. This thesis covers the study of fundamentals of antennas and microstrip patch antenna. In this thesis a two-port microstrip patch antenna system with significant isolation enhancement (60dB), which can be deployed for Full-duplex transceiver systems. To enhance the isolation between transmitter and receiver antenna a defected ground structure is used. Slots are introduced into the ground plane to create a weak field region for the basic antenna element. Further enhancement in isolation is achieved by introducing metamaterial-based superstrate by absorbing the near field component of magnetic field. Different Full-duplex configuration were carefully analyzed based on convention performance metrics which is Scattering Parameter, Gain, and Efficiency. Further the analysis is carried to designed another Full-duplex antenna at 38GHz. After that a compact circularly polarized microstrip patch antenna is designed for in-band full-duplex system but there is a compromise between the isolation and the size of antenna. This concludes the analysis of full-duplex systems that use millimeter wave antennas.

TABLE OF CONTENTS

LIST OF FIGURES

LIST OF TABLES

Chapter 1

Introduction

1.1 Background

Wireless communication systems have undergone a series of transformations, evolving from the initial generation of mobile phones with analog audio transmission. The second generation introduced digital systems, followed by the third generation, which enabled the transmission of multimedia content. The fourth generation brought about an all-IP packet switched network, facilitating the transmission of voice data, signal, and multimedia. Currently, the industry is focused on the development and deployment of 5G networks, which are succeed and surpass the capabilities of their 4G predecessors.

With the escalating demand for faster internet access and higher data rated, it has become evident that existing fourth-generation technology is insufficient to accommodate the ever-increasing number of users and their bandwidth requirement. As result, there is a need to transition to the fifth generation of wireless communication systems, which will operate on millimeter wave frequencies. Shifting to mm-wave frequencies offers several advantages, including wider bandwidth and the ability to achieve higher data rates. These frequencies possess the speed and capacity necessary for the implementation of new technologies, such as the Internet of Things (IoT), which is a significant technological trend today.

1.1.1 5G Technologies

Millimeter Wave (mm Wave): Wide bandwidths and high data rates are provided by 5G by using millimeter-wave frequencies, which are typically above 24 GHz. Although these high-frequency bands have a limited range and are more prone to signal interference from physical objects, they have the potential to support multi-gigabit rates. To solve these difficulties, sophisticated antenna systems, beamforming, and beam tracking methods are used.

MIMO (Multiple-Input Multiple-Output): Massive MIMO refers to the use of a large number of antenna elements at the base station to improve network capacity and spectral efficiency. By transmitting multiple data streams simultaneously, Massive MIMO allows for increased data throughput and better utilization of available spectrum. It also enables beamforming to focus signals towards specific user devices, improving signal quality and coverage.

Full-duplex (FD) systems: In millimeter-wave (mm Wave) technology, full duplex communication refers to the capacity to send and receive data concurrently on the same frequency band. Due to this capabilities, wireless communication systems using these high frequencies can operate more effectively and with greater capacity. The introduction of full duplex in mm Wave technology is particularly relevant due to the unique characteristics of mm Wave frequencies. Wide accessible bandwidths that can sustain extremely high data rates are available in Mm Wave bands, typically ranging from 24.25 GHz to 29.5GHz and 37GHz to 43.5GHz.

Full- duplex antenna system have garnered significant attention in the context of high data rate wireless communication system design, since they concurrently use same time/frequency slot for both transmission and reception, leading to enhanced spectral efficiency compared to their half-duplex (HD) counterparts. But in a full- duplex antenna, suppression of self-interference (interference caused by own transmitter) is the most challenging part. The self-interference cancellation level depends on the transmitted power and the channel bandwidth.

For an efficient full- duplex system, complete self-interference cancellation is necessary since it decides the throughput of the full-duplex system. Complete self- interference cancellation is achieved at various stage, at antenna stage and at analog/digital stage, but it will also make the system applicable for a high-power system.

1.2 Motivation

The primary objective of this study is to enrich the research of Full-duplex (FD) antennas operating in millimeter wave frequencies, which have gained significant popularity as a preferred option for 5G communication. Overall, the advantages of full-duplex antennas include increased capacity, improved spectral efficiency, reduced latency, and simplified network architecture, making them a promising solution for next-generation wireless communication systems.

In my further research, I discovered that full duplex antennas have been widely adopted in various application areas. However, one significant challenge in antenna characterization is the operational bandwidth. This refers to the frequency range where the reflection coefficient of antenna, represented as S11, is below -10dB.

In this research, the first step involves studying different designs of microstrip patch antennas. Afterward, the focus shifted to exploring various configurations of full-duplex that can be utilized. Thus, the proposed design can achieve acceptable range for all the key parameters such as mutual coupling(S21/S12) and satisfactory antenna parameters.

1.3 Outline of This Thesis

This thesis comprises six chapters. In Chapter 1, a comprehensive introduction is provided for millimeter wave full-duplex antennas. Chapter2 offers a brief overview of antenna fundamentals and conventional parameters used to describe antenna performance. Chapter 3 provides a general introduction to microstrip patch antennas and their basic characteristics. Chapter4 extensively discusses the working spectrum of millimeter waves, full-duplex antenna, isolation techniques, and includes a literature survey. Chapter 5 focuses on the proposed design, which is a single band full-duplex antenna, along with the corresponding results. Finally, Chapter 6 concludes the thesis and presents future research directions.

Chapter 2

Fundamental Parameters of Antenna

To provide a comprehensive overview of antenna performance, it is necessary to define several fundamental parameters. These parameters, which include mutual coupling, antenna bandwidth, gain, directivity, and radiation pattern, are outlined below along with their corresponding descriptions.

2.1 Radiation Pattern

The radiation pattern of an antenna refers to the spatial distribution of electromagnetic energy it emits or receives. It describes how the antenna's signal is distributed in different directions in three-dimensional space. The radiation pattern of an antenna is also referred to as the antenna pattern or far-field pattern. As a result, the antenna design depicts how power is spread in space. Azimuth plane pattern and elevation plane pattern are two types of radiation patterns that can be drawn in a 2D plane for varied azimuth and elevation angles. There is different type of antenna radiation pattern which are described below:

2.1.1 Isotropic Radiation Pattern

A hypothetical lossless antenna having equal radiation in all directions. However, there are no truly isotropic antennas. Ongoing research is focused on developing quasi-isotropic antennas that approximate the ideal isotropic radiation pattern. In order to compare and assess the performance of various antennas, the idea of an isotropic antenna is used as a standard.

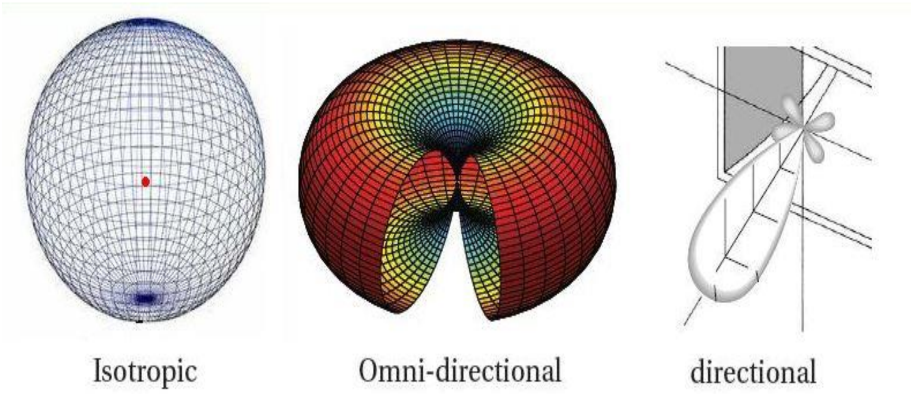

(a) (b) (c)

Figure 1. Represents (a) isotropic radiation pattern, (b) omni-directional radiation pattern, (c) directional radiation pattern of an antenna.

2.1.2 Omni-directional Radiation pattern

An antenna having an essentially non directional pattern in each plane (e.g., in azimuth) and a directional pattern in any orthogonal plane. An antenna that distributes its signal uniformly and evenly in all directions, especially in the horizontal plane, is said to be omnidirectional. Dipole, monopole, slot, and normal mode helical antennas are a few examples of omnidirectional antennas. An omnidirectional antenna emits radiation in the form of a doughnut.

An omnidirectional antenna with a larger gain is produced by reducing the emission pattern of the antenna in the vertical plane. This also concentrates more energy in the horizontal plane. As a result, antennas with narrower beams in the vertical plane can provide greater gains. Different omnidirectional antenna designs can be created with various gain values.

In the vertical plane, a 0dB gain antenna will radiate more effectively. Devices like mobile phones, cell phones, FM radios, walkie-talkies, wireless computer networks, cordless phones, GPS, wi-fi networks, Bluetooth devices.

2.1.3 Directional Radiation pattern

An antenna having the property of radiating or receiving more effectively in some directions as compared to other directions. For point-to-point applications like satellite communication and in base station antennas for sector coverage, they are frequently utilized. The Yagi, log-periodic, horn, panel antenna are a few examples of directional radiation pattern.

2.2 Directivity

An antenna's directivity informs us of how concentrated or focused its energy is in a specific direction. It is crucial for an antenna to have strong directivity when receiving signals. Like an isotropic antenna, an antenna with a directivity of 1 (or 0dB) radiates energy uniformly in all directions. By comparing the radiation intensity coming from the antenna in a particular direction to the average radiation intensity coming from all directions, directivity is computed. The total power radiated divided by 4π is the average radiation intensity. Therefore, the directivity is the ratio of the radiation intensity of an isotropic antenna to that of a non-isotropic antenna in a certain direction.

$$\boxed{D = \frac{U}{U_0} = \frac{4\pi U}{P_{rad}}}$$

If a specific direction is not mentioned, the direction with the highest radiation intensity (maximum directivity) is determined as follows.

$$\boxed{D_{max} = D_0 = \frac{U|_{max}}{U_0} = \frac{U_{max}}{U_0} = \frac{4\pi U_{max}}{P_{rad}}}$$

D = Directivity (dimensionless)

D_o = maximum Directivity (dimensionless)

U = radiation intensity (W/unit solid angle)

U_{max} = maximum radiation intensity (W/unit solid angle)

U_o = radiation intensity of isotropic source (W/unit solid angle)

P_{rad} = total radiated power (Watt)

2.3 Gain

This is another performance characteristic that is closely related to efficiency and directional capabilities of antenna. It is also referred as power gain. It indicates how well a transmitting antenna can emit a certain amount of power into space in a specific direction. In the case of a receiving antenna, it indicates how successfully the antenna converts electromagnetic waves received into electrical power. It is usually expressed in decibels (dB).

$$\boxed{\text{Gain} = \text{efficiency} \times \text{directivity}}$$

It is referred to as Power Gain when it is calculated with efficiency Eantenna and directivity D.

Power Gain = Eantenna. D

The term "Directive Gain" refers to the directivity that is delivered in a specific direction.

2.4 Antenna Efficiency

An antenna's ability to convert electrical power into radiated power or vice-versa is known as its efficiency. It measures the antenna's energy loss or conversion efficiency. The overall antenna efficiency takes into the following losses:

(i) Reflection mismatch between transmission line and the antenna

(ii) Conductor and dielectric losses.

$$\boxed{\eta_r = \frac{P_{rad}}{P_{in}}}$$

P_{rad}: Total power radiated by an antenna

P_{in}: Total input power accepted by the antenna from transmission line.

2.5 Mutual Coupling

In antenna systems, the phenomena of numerous antennas in a proximity influencing one another's performance are known as mutual coupling. It develops as a result of electromagnetic waves from one antenna impacting surrounding antennas. Electromagnetic fields from adjacent antennas interact with one another when they are near together. Several outcomes of this interaction are possible, including Radiation pattern distortion, Gain reduction, Impedance mismatch, Frequency shifting, Crosstalk and interference.

The individual elements' reflection coefficients and mutual coupling parameters constitute the scattering matrix[S]:

Mutual coupling: $s_{ij} = \frac{b_i}{a_i}\Big|_{a_k=0 \; for \; k \neq j}$

$$\begin{bmatrix} b_1 \\ b_2 \\ b_3 \\ b_4 \\ b_5 \end{bmatrix} = \begin{bmatrix} S_{11} & S_{12} & & & S_{15} \\ S_{21} & & & & S_{25} \\ S_{31} & & & & \\ & & & & \\ S_{51} & & & & S_{55} \end{bmatrix} \begin{bmatrix} a_1 \\ a_2 \\ a_3 \\ \\ a_5 \end{bmatrix}$$

2.6 Antenna Bandwidth

Another essential antenna component is antenna bandwidth, which is defined as the range of frequencies that the antenna can operate successfully without significant degradation in performance. There are many ways to describe bandwidth, including gain, axial ratio, impedance, and VSWR bandwidth. The frequency range where the antenna's input impedance is suitably matched to the characteristic impedance of the feeding transmission line is known as the impedance bandwidth. The upper to lower frequency ratio of the desired operation is used to represent the bandwidth for broadband antennas.

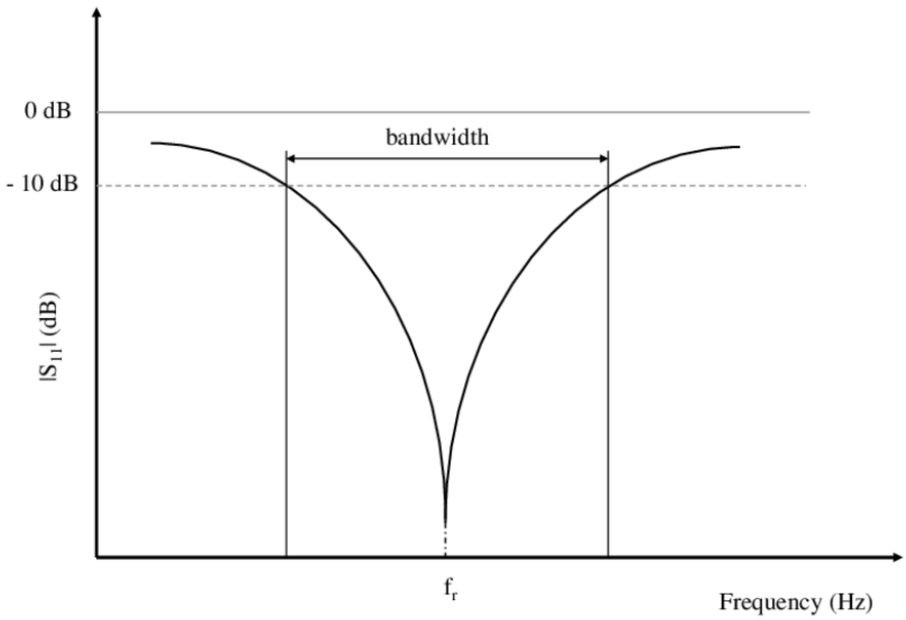

Figure 2. S Parameter Plot (Return Loss Plot) Bandwidth for $S_{11} < -10$ dB.

Chapter 3

Microstrip Patch Antennas

3.1 Introduction

A microstrip Patch antenna is having a simple configuration consisting of two thin metallic layers separated by a dielectric substrate. The top layer acts as a radiating patch, while the ground layer is formed by the bottom layer. Typically, copper is used as the metallic layer, although gold may also be utilized. The patch can have various shapes, such as rectangular, triangular, circular, square, dipole, or elliptical. The choice of patch shape depends on factors like fabrication convenience and the ability to analyze and predict the antenna's performance accurately.

With a dielectric constant ranging from $2.2 \leq \varepsilon_r \leq 12$, a variety of dielectric materials are available for building microstrip antennas. A critical factor in defining the properties of the antenna is the substrate thickness, commonly referred to as the dielectric thickness.

Loosely bound fields are made possible by thicker substrates with lower dielectric constants, increasing efficiency and bandwidth. This, however, results in a bigger antenna element size. Contrarily, closely bound fields are encouraged by thinner substrates with higher dielectric constants, which reduces unwanted radiation and coupling. Although this results in reduced antenna element sizes, it may also cause higher losses and a narrower bandwidth.

As a result, achieving optimal antenna performance and striking a balance between the antenna size and circuit design are never mutually exclusive. To achieve the ideal balance for a particular application, designers must consider the desired antenna properties, available substrate materials, dielectric constants, and substrate thickness.

3.2 Basic Characteristics

The performance of an antenna is not only determined by its design but also by the combination of the antenna and the transmission line it is connected to. Microstrip antennas typically have a complex input impedance, while the characteristic impedance of the transmission line is usually a real value, commonly 50 ohms. This impedance mismatch leads to a phenomenon called voltage standing wave, resulting in poor impedance bandwidth.

Impedance matching techniques are used to solve this problem. Impedance matching networks are used in these methods to connect the antenna and transmission line. The objective is to minimize reflections and maximize power transfer by matching the complex impedance of the antenna to the actual impedance of the transmission line.

Impedance matching techniques come in various forms, and one commonly used approach is circuit theory. In order to match the characteristic impedance of the transmission line, it entails building circuits that change the impedance sensed by the antenna. By doing this, the antenna performs more effectively, the mismatch is decreased, and the performance in terms of bandwidth and power transfer is improved.

3.3 Basic formula of a microstrip patch antenna

Width of the patch (W_p)	$W_p = \dfrac{c}{2 \times f_r \times \sqrt{\dfrac{\varepsilon_r + 1}{2}}}$
Length of the patch ($\mathrm{L_p}$)	$\mathrm{L_p} = \mathrm{L_{peff}} - 2 \times \Delta_{\mathrm{L_p}}$
Width of the Substrate (W_g)	$W_g = 6\mathrm{h} + W_p$
Length of the Substrate (L_g)	$L_g = 6\mathrm{h} + L_p$
Width of the feed (W_f)	$W_f = \dfrac{7.48 \times h}{e^{\left(z_0 \times \sqrt{\frac{\varepsilon_r + 1.41}{87}}\right)}} - 1.25 \times t$
Length of the feed (L_f)	$L_f = \dfrac{1}{4} \lambda_g$

Where,

h = height of the substrate, t = ground thickness, ε_r = relative permittivity of dielectric substrate, c = speed of light, f_r = resonant frequency, z_0 = input impedance:50Ω, λ_g = guided wavelength, Δ_{L_p} = length extension, L_{peff} = effective length.

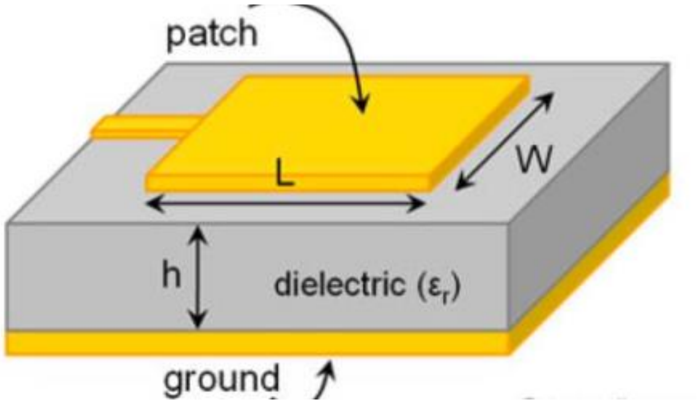

Figure 3. Basic Diagram of a patch antenna.

3.4 Radiation Mechanism

In general, a microstrip patch antenna radiates primarily in the broadside direction, which is perpendicular to the patch surface. However, depending on the design and arrangement, some radiation may also happen in off-broadside directions, resulting in additional lobes in the radiation pattern.

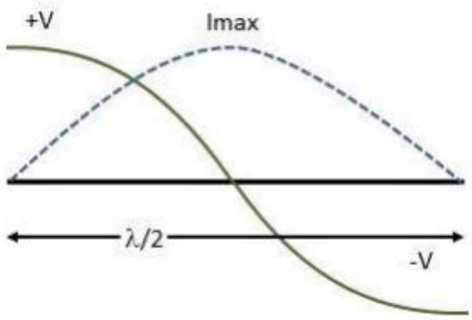

Figure 4. Current and voltage variation along the patch length.

To comprehend the radiation-causing mechanisms of microstrip antennas consider a rectangular antenna with a microstrip feed line and a radiating patch that is half a wavelength long. You can think of a rectangular antenna as an open-ended microstrip line that receives energy from the other end. The current should be zero at the corners (at the beginning and end) and maximal in the centre because the patch is half a wavelength long and open ended on the other side. Voltage and current will be 90 degrees out of phase. The voltage will be at its highest positive point at the beginning of the patch and at its highest negative point at the end.

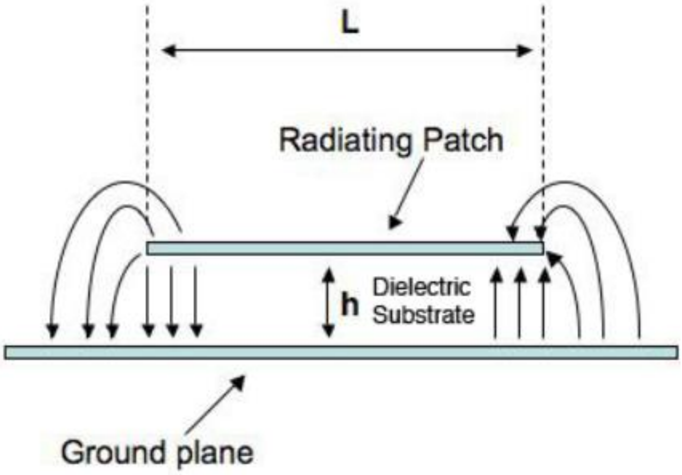

Figure 5. Fringing Fields.

The microstrip antenna can be visualised as a rectangular cavity with open sidewalls. The radiation is produced by the fringing fields through the open sidewalls. Fields lines, as indicated in the above illustration, are underneath the patch and point in the opposite direction of the corner. There is no sudden end to this field line. The field lines form a bow, and the corners are built with bordering fields. As the bordering field bows, the radiation rises. Thus, we may state that fringing fields are what induce the emission from microstrip antennas.

3.5 Feeding Techniques

There are several methods available for feeding a microstrip antenna, and the choice of feeding technique depends on various factors related to the antenna design. The primary consideration is achieving effective power transfer from the feed line to the radiating element of the antenna, which requires proper matching between the feed and the antenna.

It is preferable for the input impedance of the antenna to match the input impedance of the majority of RF and microwave sources, which is 50 ohms. The antenna interacts with free space, which causes it to serve as an impedance transformer between the source's impedance of 50 ohms and that of free space, which is roughly 377 ohms.

Microstrip antenna feeding methods can be broadly divided into two groups: contacting and non-contacting feeding. In contacting feeds, the feed line is directly attached to the antenna's radiating patch, allowing RF power to be provided to it directly. Microstrip line feed and coaxial probe feeding are two examples.

On the other side, non-contacting feeding techniques use electromagnetic coupling to feed RF power indirectly. Aperture coupling and proximity coupling are two frequently employed non-contacting coupling techniques. In order to establish electromagnetic coupling, proximity coupling includes positioning a coupling element close to the radiating patch, as opposed to aperture coupling, which couples the energy from the feed line to the radiating element through a small aperture or slot.

3.5.1 Microstrip Line Feeding

The microstrip line feed is the feeding method for microstrip antennas that is most frequently used. This technique involves producing the feed line on the same substrate as the radiating patch, but with a conducting strip that is narrower than the patch. This design allows for a planar structure and easy construction. The microstrip line feed offers the advantage of simplicity and compatibility with impedance matching techniques. It is straightforward to implement and allows for effective impedance matching between the feed line and the antenna.

The possibility of spurious feed radiation is one disadvantage of the microstrip line feed, though. This means that some RF power may unintentionally radiate from the feed line, which could have an adverse influence on the performance of the antenna.

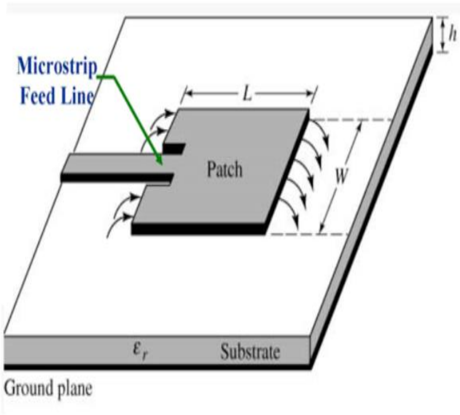

Figure 6. Microstrip Line Feed.

3.5.2 Coaxial Feeding

In this type of feeding technique patch is fed by co-axial cable. It is a non-planar feeding technique. In this method of feeding, the outer cable is linked to the ground and the coaxial cable core is soldered directly to the patch. The core conductor is inserted into a hole in the substrate.

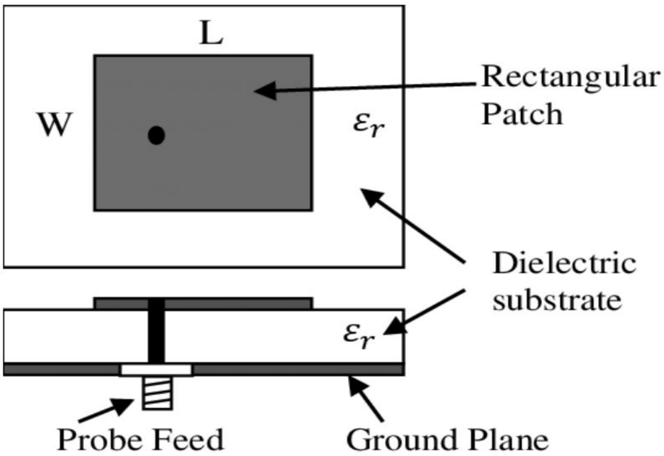

Figure 7. Coaxial Feed Line.

The main advantage of this feeding approach is that the inner conductor can be fed directly to the feed point where the input impedance is equal to the characteristic impedance of the feed line. Additionally, the ground plane separates unwanted radiation from the feed and antenna radiation, enhancing radiation performance.

3.5.3 Proximity Feeding

Two types of dielectric substrates are used in this non-contacting feeding approach. The open-ended microstrip line that is wedged between the two substrates and is not directly connected to the patch. Electrically connected to the emitting patch is the energy from the feed line.

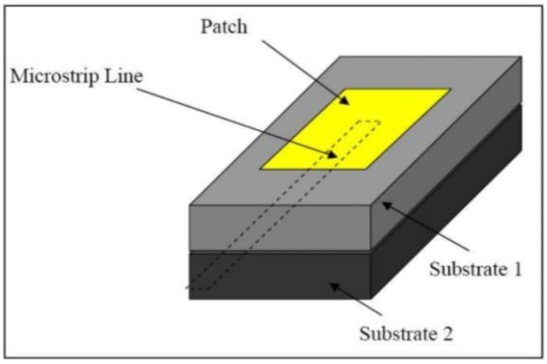

Figure 8. Proximity Feed.

Below the patch, at a lower level, the feed line is moved. At a point where the antenna input impedance is 50 ohms, the feed ends. This technology enabled planar feeding and significantly decreased feed line radiation by shifting the feed line to a lower level. Additionally, compared to previous techniques, it is easier to predict, has a lower quantity of spurious feed radiation, and has a higher bandwidth efficiency. This technology's drawbacks include the need for multi-layer manufacturing and the low polarisation purity it offers.

3.5.4 Aperture Coupled Feed

Two different types of dielectric substrates are used in this kind of feeding technique: an antenna dielectric substrate and a feed dielectric substrate. A ground plane with a slot in the middle is sandwiched between these two substrates. On top of the antenna substrate is positioned the metal patch. The ground plane is located on the opposite side of the dielectric antenna. The location of the feed line and feed dielectric on the opposite side of the ground plane creates isolation.

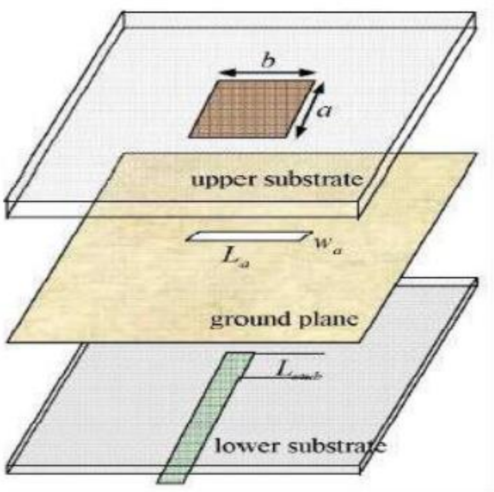

Figure 9. Aperture Coupled Feed Line.

For the upper substrate, a thick substrate with a low dielectric constant is used to achieve good radiation and bandwidth. While when the upper substrate is made of a thin, high-dielectric-constant material this enables effective energy transfer from the feed line to the patch. The patch slot should be situated where the magnetic field is strongest to get the best coupling between the feed structure and the patch slot. When compared to microstrip and coaxial probe feeding, this method of feeding has greater polarization purity, lower spurious feed radiation, and a larger bandwidth.

Chapter 4
Millimeter Wave Full-Duplex Antennas

4.1 Introduction to Millimeter Wave Spectrum

The effective use of the electromagnetic spectrum is one of the most important considerations in modern electronics development. It is challenging and crucial to manage and distribute the spectrum among the many application areas due to the constantly growing number of devices and their reliance on the spectrum. Since the current cellular band is in the 800–2100MHz range, moving to the band of 30–300GHz will alleviate the spectrum overcrowding that exists today. As a result, millimeter wave systems come to the rescue in this regard due to their location in the electromagnetic spectrum and their ability to provide significant relief on that issue. For wireless communication to achieve faster data speeds, spectrum is a determining element. The desire for greater bandwidth rises proportionately to the rise in the demand for faster data transfer rates.

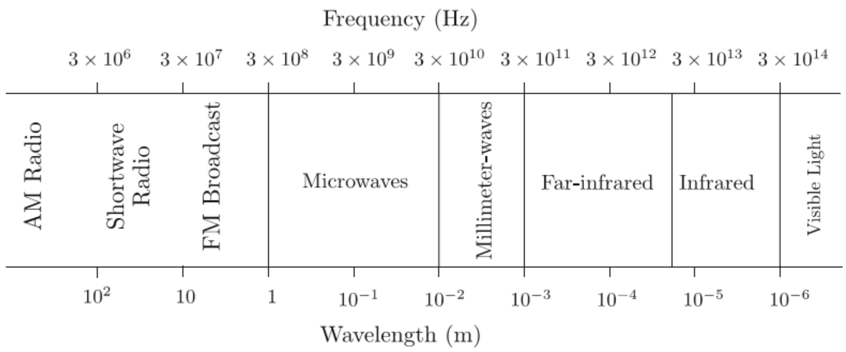

Figure 10. Electromagnetic Spectrum.

The wavelength range of the millimetre wave spectrum typically ranges from 10 to 1 mm. The relationship between bandwidth and symbol rate in communication systems is that the faster the data transfer, the greater the bandwidth. This indicates that larger data rates will be possible from communication systems operating at higher frequencies. This can be understood as a 1 percent bandwidth of 30GHz being equal to 300MHz being equal to 3MHz. Therefore, working with millimetre waves can be regarded beneficial.

4.2 Millimeter Wave Antennas

The transition to the millimeter wave region is influenced by several important factors. Among these, there is a common misconception that propagation losses exclusively rely on frequency, implying that signals with higher frequencies do not propagate as well as those with lower frequencies. It should be mentioned, nevertheless, that this misunderstanding is not totally true. This misunderstanding results from the underlying assumption that the path loss between two isotropic antennas, or $\lambda/2$ dipoles, is calculated at a specific frequency. Since the effective aperture area of these antennas increases with wavelength and decreases with carrier frequency, it follows that an antenna with a larger aperture will have a higher gain than one with a smaller one because it will be able to absorb more energy from an approaching radio wave. However, working on shorter wavelengths (higher frequencies) than longer wavelengths (lower frequencies) does not have any inherent disadvantages in terms of free space loss because more antennas can be placed in the same space with shorter wavelengths (higher frequencies), and this large number of antennas also enables transmitter and receiver beamforming with high gain.

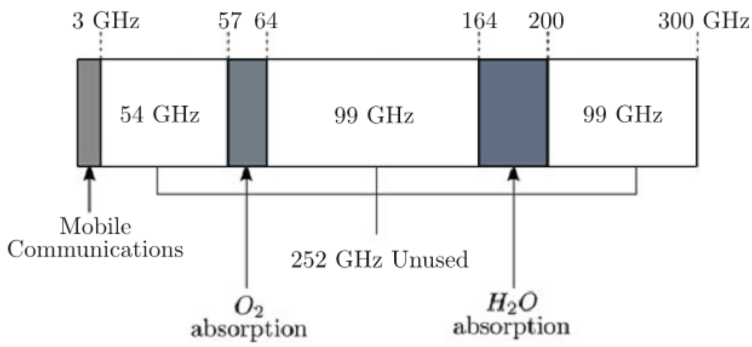

Figure 11. Millimetre Wave Frequency Bands.

A perfect option for millimeter wave antenna design is a microstrip patch antenna. Since they can emit at high frequencies and operate in two bands, microstrip patch antennas are proving to be a desirable option for 5G applications. The most popular substrates include Teflon, RT Duroid (Rogers), FR4 epoxy, and Roger (RO4003). The selection of the substrate and its height are crucial. The fringing fields and consequent radiation rise together with the substrate's height. When designing an antenna, the patch's dimensions and shape are crucial factors to consider. A microstrip patch antenna can have several shapes. The surrounding fields are shaped by the patch. It is also possible to increase the antenna's gain by varying the patch's shape. The millimeter-wave antenna would be modest since the relationship between the frequency of operation and antenna size is inverse.

4.3 Introduction to Full-Duplex System.

Full-duplex (FD) antenna systems have drawn a lot of attention in the context of high data rate wireless communication system, because they simultaneously use the same time/frequency slot for both transmission and reception, doubling spectral efficiency as well as it leads to the more efficient use of the Rf spectrum compared to the conventional half duplex (HD) system.

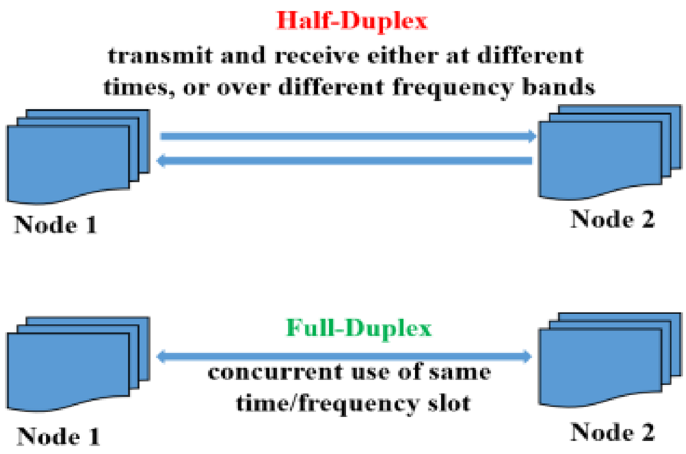

Figure12.Schematic representation of a FD and HD Wireless Communication System.

The main issues with full-duplex antennas are bandwidth and self-interference cancellation. Self-interference is the unwanted signal produced by the same In band full duplex (IBFD) terminal's transmitter port (Tx) that obstructs the desirable signal at the receiver port (Rx). The transmission power (Pt) and the received noise power (PN) are the two factors that affect SIC the most.

PN = - 174dBm +10* log (BW) +NF.

Where -174 dBm is the reference noise power per 1 Hz at room temperature.

For example, PN is equal to -80 dBm for a 50 MHz BW and a 17 dB noise figure. An SI cancellation of 20 dBm - (-80dBm) = 100 dBm is required to suppress RF leakage for a radio transceiver with 20 dBm Tx power (Pt).

4.4 Literature Survey on Full- Duplex Antenna.

The transition from fourth generation (4G) to fifth generation (5G) mobile communications ushers in a time of ubiquitous connectivity, extremely high radio capacity, and low latency. In addition to boosting network capacity, 5G is anticipated to achieve a peak data speed of 20 Gbps by opening a new swath of airwaves in the millimeter-wave (mm-wave) range from 30 to 300 GHz. mm-wave 5G antennas are anticipated to have high gain and efficiency values as well as wide bandwidths.

4.4.1 Survey 1

In this letter, an in-band full-duplex application using a single-layer compact co-polarized shorted TM1/2,0 mode microstrip patch antenna is proposed. By combining the resonances of a patch antenna and a quarter-wavelength microstrip line, the wideband behavior of the patch antenna is obtained. Slots are used to generate a weak field zone, and the reception antenna is then positioned there. As a result, isolation is increased to 22 dB in the -10 dB impedance bandwidth. With the addition of T-shaped metallic strips, isolation is increased to 25 dB across the board, with a peak isolation of 36 dB at 2.46 GHz. The advantages of the proposed antenna structure include its small size, low profile, extremely simple feed, and planar layout, making it potentially useful for simultaneous transmit and receive antenna systems that are compact and planar-integrated.[2].

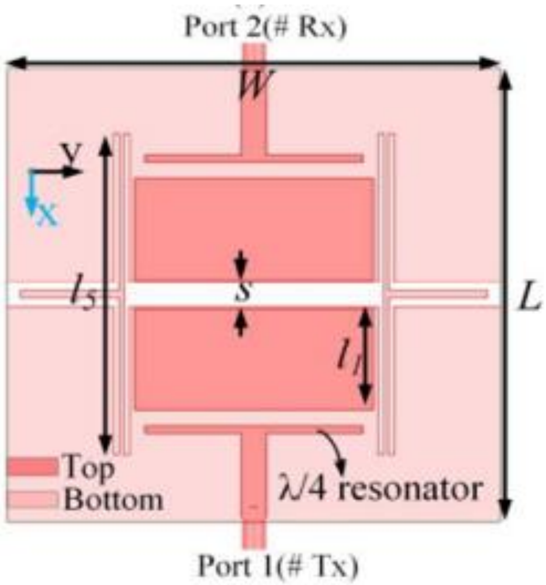

Figure 13. Antenna Geometry.

Top view with design parameters (in mm): L = 90, W = 95, S = 6, w_f = 4.9, l_1 = 20, l_2 = 18.55, l_4 = 19, l_5 = 64.5, g = 3.4, g_1 = 5.5, g_2 = 2.8, w_1 = 46, w_2 = 1.6, and w_3 = 1.

The proposed structure is designed on low-loss RT Duroid (Rogers) substrate with εr = 2.2, loss tangent (tanδ) of 0.0009, and height of 1.57 mm. The dielectric substrate has the dimension of 90 mm×95 mm (L× W). The structure was designed and optimized at every stage using ANSYS Electronics Desktop (HFSS).

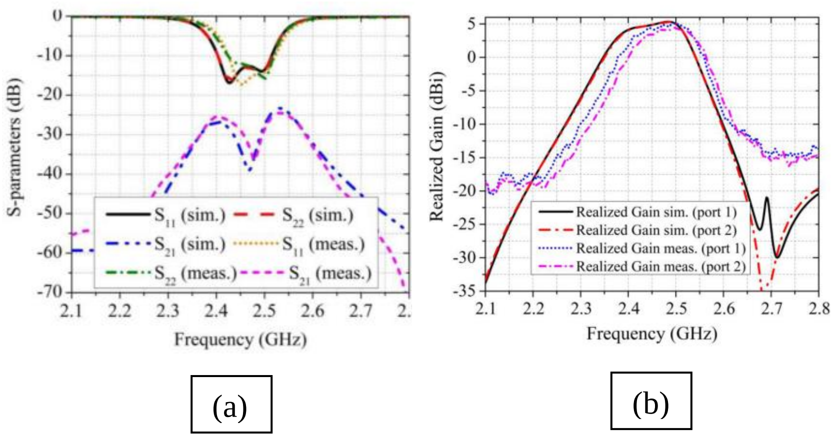

Figure 14. S-parameter Plot (a) and Gain Plot (b) for Above Design.

4.4.2 Survey 2

In this letter, we offer a colinearly polarised in band full-duplex (FD) microstrip antenna system that achieves extremely high inter-port isolation using passive self-interference cancellation.

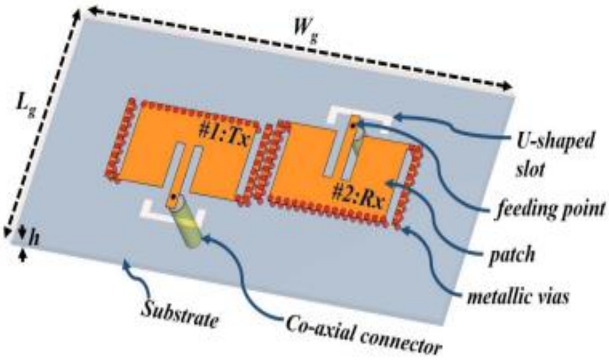

Figure 15. Three-dimensional perspective view of the proposed two element FD antenna.

The proposed two-element FD antenna has overall dimensions of ($L_g \times W_g \times h$) 38 mm × 80 mm ×1.6 mm and was designed on an RT-Duroid 5880 substrate ($\varepsilon_r = 2.2$, $\tan\delta = 0.0009$).

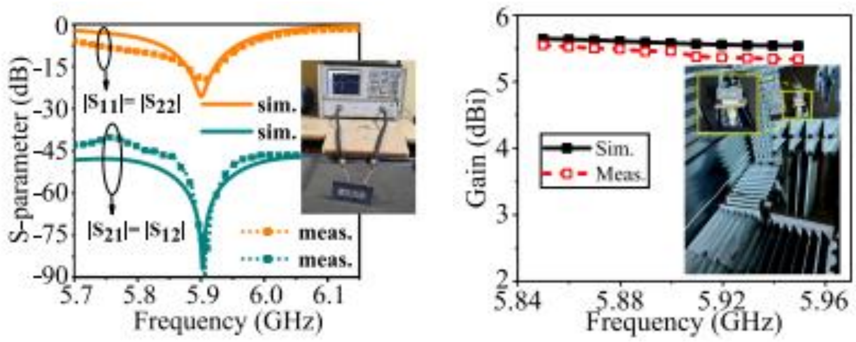

(a)

(b)

Figure16. S-parameter Plot (a) and Gain Plot (b) for Given Design.

The proposed FD antenna employs a new combination of 1) field confinement near individual antennas due to metallic vias, and 2) U-shaped slots etched from the ground plane to achieve this isolation increase without the usage of any circulator, hybrid, or complex feed-network. With a broadside gain of 5.63 dBi and an X-pol level of less than 20 dB, the proposed FD antenna exhibits inter-port isolation values of >54 dB over the operating band of 5850–5945 MHz and 90 dB at 5.9 GHz.[3].

4.4.3 Survey 3

In this study, we suggest a full-duplex transceiver system that can be implemented with a closely spaced, two-port microstrip patch antenna system that has a large isolation improvement (> 90 dB).

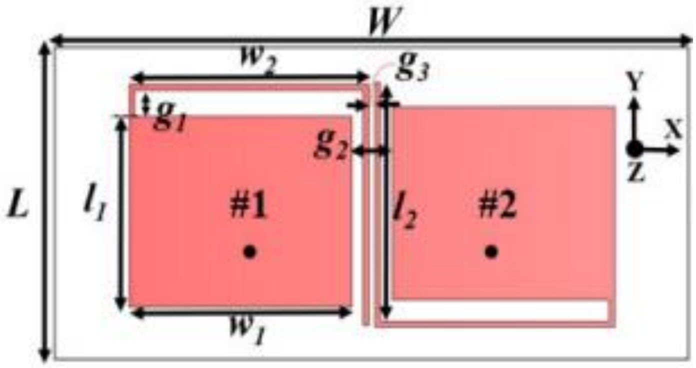

Figure 17. Antenna Geometry.

Proposed two-port antenna showing dimensions: L = 1.092λ0, W = $0.507\lambda_0$, $l_1 = 0.31\lambda_0$, $w_1 = 0.38\lambda_0$, $l_2 = \lambda_0$, $w_2 = 0.4\lambda_0$, $g_1 = 0.039\lambda_0$, $g_2 = 0.068\lambda_0$, $g_3 \approx 0.01\lambda_0$, $l_d = 0.394\lambda_0$, $w_d = 0.117\lambda_0$, $l_s = 0.478\lambda_0$,$w_s = 0.018\lambda_0$, $g_s = 0.00429\lambda_0$, $h_1 = 0.0057\lambda_0$, $h_2 = 0.0136\lambda_0$, $h_3 = 0.03\lambda_0$. At 5.85 GHz, and was designed on a RTD5880 substrate of 1.57 mm thickness, having $\varepsilon_r = 2.2$ and tan $\delta = 0.0009$. We place a two-port microstrip patch antenna system in close proximity to a resonant combination of a rectangular defective ground structure (DGS) and a near-field decoupling structure (NFDS).

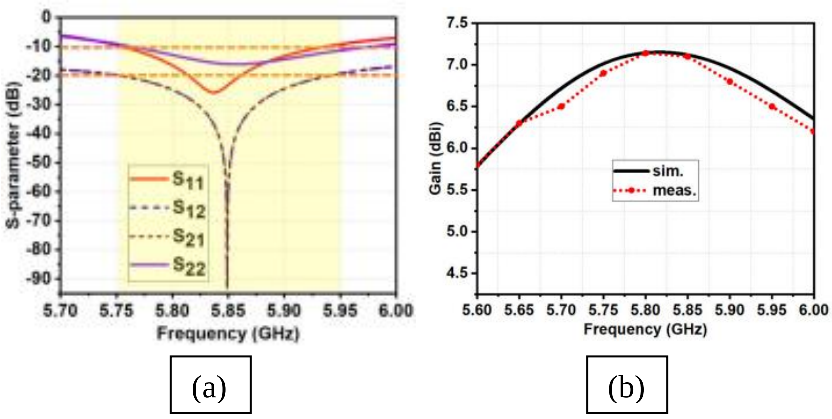

Figure 18. S-parameter Plot (a) and Gain Plot (b) for Given Design.

This significantly lowers the port-to-port mutual coupling (< -90 dB), which can aid in self-interference cancellation for full-duplex point of view without the use of additional circuitry and still maintain desirable impedance matching performance (< -15 dB). Individual antennas have gains greater than 7 dBi and radiation efficiencies greater than 97% (antenna overall efficiency is provided for FD at 5.85 GHz (higher WLAN frequencies and 5G NR-U band).[4]

4.4.4 Survey 4

In-band full-duplex (IBFD) 2.4 GHz antenna with good isolation is described in this study.

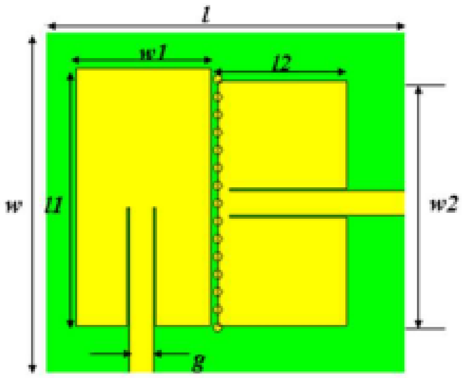

Figure 19. Antenna Geometry.

Proposed antenna including dimensions: Top view dimensions: $w = l = 0.352\lambda_0$, $w_1 = 0.128\ \lambda_0$, $l_1 = 0.244\ \lambda_0$, $w_2 = 0.232\ \lambda_0$, $l_2 = 0.123\ \lambda_0$, $g = 0.024\ \lambda_0$, $g_1 = 0.017\ \lambda_0$, $r = 0.004\ \lambda_0$, $g_2 = 0.0032\ \lambda_0$ and was designed on FR4 (relative permittivity $\varepsilon_r = 4.3$, $\tan\delta = 0.025$) substrate of 0.8mm thickness to resonate at 2.4 GHz. A typical inset-fed microstrip antenna is one of the antennas. A quarter-wavelength inset-fed microstrip antenna serves as the secondary antenna. By positioning cylindrical metal vias along one of its radiating edges, the quarter-wave patch is created. The suggested IBFD antenna structure is more compact than other documented structures since the two antennas are orthogonally positioned with a $0.0032\ \lambda_0$ inter-element separation. Inter-port isolation of 36 dB is attained.[5]

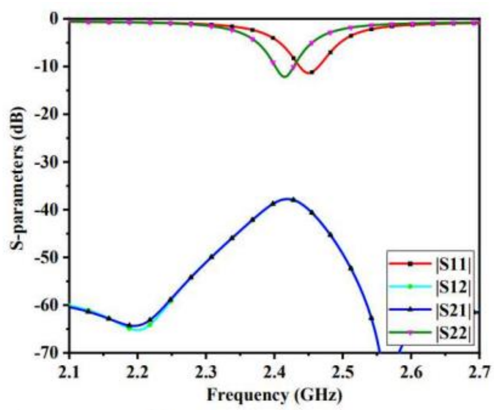

Figure 20. S-parameter Plot for Given Design.

4.4.5 Survey 5

This work proposes an in-band full-duplex microstrip antenna with strong T_x-R_x isolation that is based on a co-linearly polarized shared radiation.

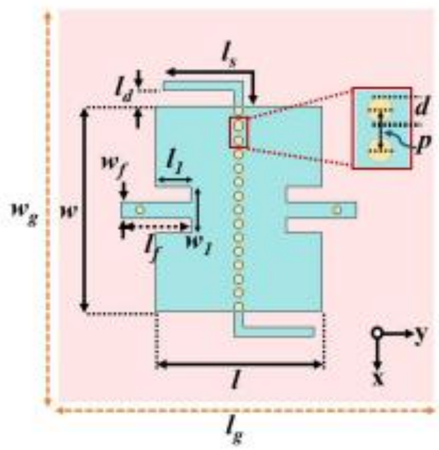

Figure 21. Antenna Geometry.

Top view of the proposed SR-FD antenna. Dimensions: $w_g = 1.024\lambda_0$, $l_g = 0.841\lambda_0$, $h = 0.031\lambda_0$, $l_s = 0.222\lambda_0$, $l_d = 0.033\lambda_0$, $l = 0.353\lambda_0$, $w = 0.432\lambda_0$, $l_1 = 0.075\lambda_0$, $w_1 = 0.098\lambda_0$, $w_f = 0.034\lambda_0$ (where λ_0 represents the free-space wavelength at 5.9 GHz) and is designed on an RT-Duroid 5880 substrate ($\varepsilon_r = 2.2$, $\tan\delta = 0.0009$ having $l_g \times w_g \times h$ ($0.841\lambda_0 \times 1.024\lambda_0 \times 0.031\lambda_0$. The T_x and R_x terminals of the proposed FD antenna are designed on a single patch, which results in high T_x R_x isolation (60 dB), with a series of vias loaded in the patch's middle line and two L-shaped stubs at either end.

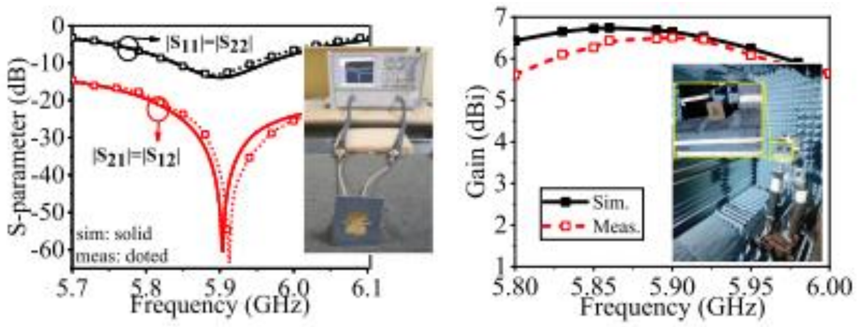

(a) (b)

Figure 22. S-parameter Plot (a) and Gain Plot (b) for Given Design.

The proposed SR-FD antenna exhibits 60.8 dB T_x-R_x isolation at the operational frequency of 5.9 GHz. With a peak realized gain of 6.65 dBi and co-to-cross polarization isolation > 18 dB, the T_x and R_x terminals of the FD antenna display identical radiation properties.[6]

4.4.6 Survey 6

For wireless local area network (WLAN) applications, a dual-band, dual-polarized in-band full-duplex antenna with good isolation performance is described. To improve the isolation, a neutralization line is connected between the grounds of the transmitter (T_x) and receiver (R_x) antennas.

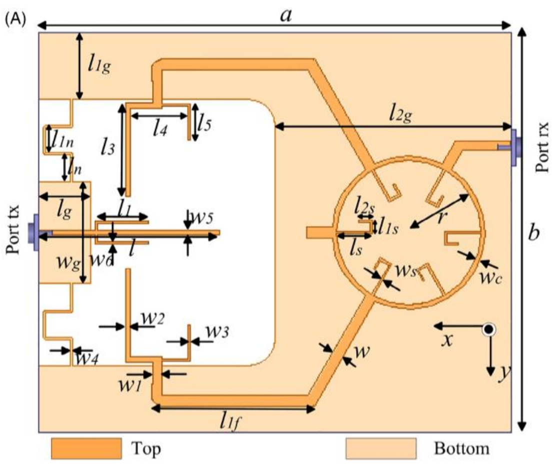

Figure 23. Antenna Geometry.

Schematic diagram of the proposed structure. Geometrical parameters: a = 106, b = 90, l = 40.5, r = 16.2, w_c = 1, w = 2.4, l_1 = 12.3, l_3 = 21, l_4 = 13.05, l_5 = 8, w_g = 23, l_{1f} = 36.4, l_g = 11.5, l_{1g} = 15, l_{2g} = 53, w_1 = 2, w_2 = 1.1, w_3 = 0.5, w_4 = 0.5, w_5 = 0.8, w_s = 0.45, w_6 = 0.5, l_s = 8.1, l_{1s} =

3, l_{2s} = 3, l_n = 6, l_{1n} = 6 (all values are in mm) and was designed on a substrate Taconic TLY (ε_r = 2.2, tanδ = 0.0009) with a thickness of 0.78 mm. By utilizing a 180-ring hybrid coupler between the receiving antenna parts, isolation is further improved. The 180-ringhybrid coupler's differential ports are used to feed the receiving antenna elements, which are arranged in opposition to one another for improved isolation.

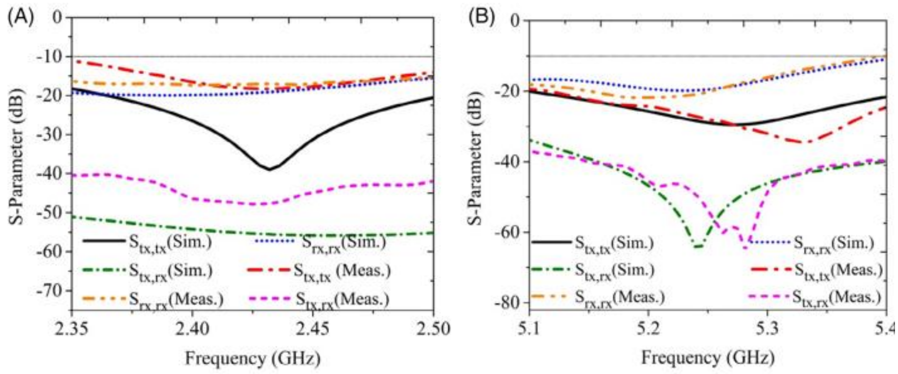

Figure 24. Measured and simulated S-parameters of the proposed structure (A) 2.44 GHz frequency band and (B) 5.25 GHz frequency band.

The measured maximum isolation between the ports is 48 dB and 63 dB, respectively, while the simulated inter-port isolation is 55 dB and 62.5 dB at 2.44 GHz and 5.25 GHz, respectively.

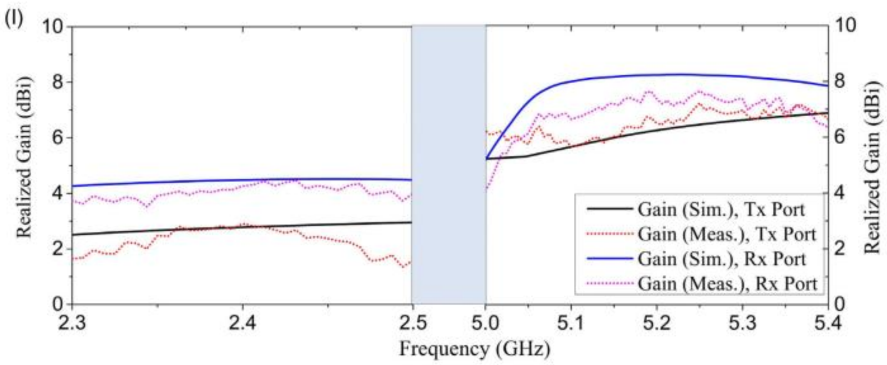

Figure 25. simulated and measured realized gain for port Tx excitation and port Rx excitation.

For the transmitting port, the simulated realized gain is 2.8 dBi at 2.44 GHz and 6.3 dBi at 5.25 GHz.

4.4.7 Survey 7

In this study, we suggest a small co-linearly polarized microstrip antenna for in-band full-duplex systems that has a low profile and identical radiation parameters.

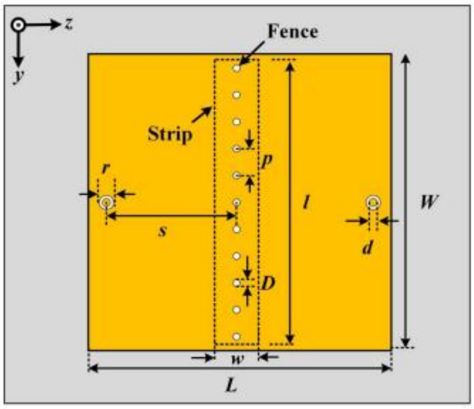

Figure 26. Antenna Geometry.

The suggested antenna employs only F4BM dielectric substrates, with $\varepsilon_r = 2.65 \pm 0.05$ and $\tan\delta = 0.002$. The two dielectric substrate layers are the same size as the metallic ground in terms of $L_g \times W_g$ (150 mm×150 mm). When the FSR resonates, the radiating current is concentrated on the half part of the patch, performing at its half-TM10 mode with high port isolation. The proposed FSR is composed of a metallic vias fence and a strip with a distance from the ground, acting as a pair of distributed inductor and capacitor. A prototype with the size of $0.25\lambda_0 \times 0.25\lambda_0 \times 0.04\lambda_0$ (λ_0 is the free space wavelength at the centre frequency) has been constructed and tested to confirm the suggested antenna.

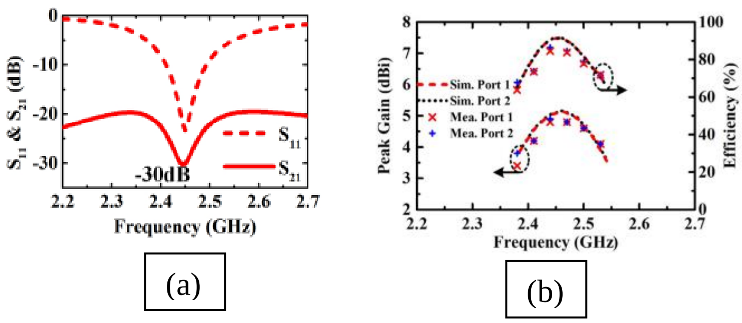

Figure 27. S-parameter Plot (a) and Gain Plot (b) for Given Design.

Within the 2.40–2.52 GHz operational bandwidth, the measured findings show a high isolation of better than 20 dB and a maximum of

30 dB. Over the operational bandwidth, the realized peak gain is greater than 4.1 dBi, with the highest value of 4.9 dBi attained at 2.46 GHz. Within the operating bandwidth, the T_x and R_x ports, respectively, achieve observed antenna efficiencies of over 70% and 72%, with the two ports' maximum values at 2.46 GHz being 85% and 86%, respectively. With a maximum efficiency of 92% at 2.46 GHz, the simulated efficiency is higher than 76% over the working bandwidth.[8].

4.4.8 Survey 8

In this study, a dual-polarized, proximity-fed bistatic antenna system with relatively broad self-interference cancellation (SIC) performance for 2.4 GHz single-channel full-duplex (SCFD) or in-band full-duplex (IBFD) wireless applications is presented. The described antenna system consists of two proximity-fed patches that are spatially separated by only $\lambda_0/4$ and have dual-polarized characteristics for transmit (T_x) and receive (R_x) modes. Wider impedance bandwidths (BWs) are available for both the T_x and R_x ports with proximity feeding.[9]

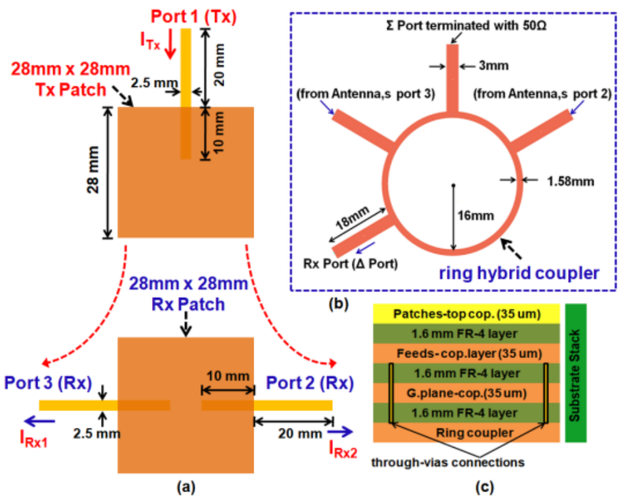

Figure 28. (a) Topology of dual-polarized, proximity-fed bistatic patch antenna system which is comprised of single-port T_x patch and two-ports R_x patch for differentially driven R_x mode operation for SIC. (b) 3 dB/180˚ ring hybrid coupler as an SIC circuit. (c) Stacked substrate.

The ring hybrid coupler and three-port antenna were each implemented on a separate FR-4 substrate with a 1.6 mm thickness (($\varepsilon_r = 4.4$ and $\tan\delta = 0.02$). A single-port, proximity-fed square patch is used to excite the

T_x mode, while a dual-port, differentially driven, proximity-fed patch is used to realize the operation of the R_x mode. The R_x ports of the patch and the differential feeding circuit are connected through vias to provide the compact structure for the antenna that is being presented.

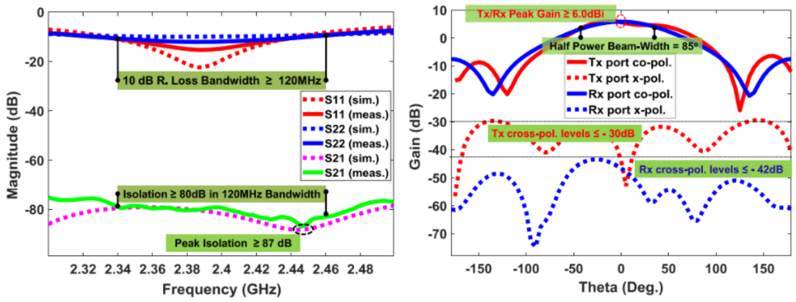

(e) (f)

Figure 29 S-parameter Plot (e) and Gain Plot (f) for Given Design.

The experimental results show higher than 80 dB inter-port isolation over the whole 10 dB return-loss, while the implemented antenna prototype characterizes better than 87 dB peak inter-port decoupling. Additionally, the reported findings offer a gain of greater than 6 dBi.

4.4.9 Survey 9

The presented antenna topology is based on four identical and sequentially rotated trimmed patches with right hand circular polarized (RHCP) characteristics, and is designed as a unidirectional, co-circularly polarized (CP), printed antenna with highly decoupled or isolated transmit (T_x) and receive (R_x) ports for 2.4 GHz in-band full duplex (IBFD) applications. Equal amounts of self-interference (SI) are produced by the symmetrical positioning of two T_x patches with regard to both R_x elements, which was inhibited through balanced stimulation of T_x mode. At every R_x patch, this method effectively suppresses SI. A second balanced feeding network installed at the R_x port of the proposed antenna architecture substantially reduces the residual SI.[10].

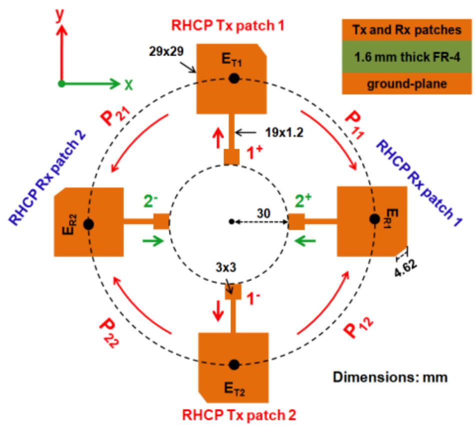

Figure 30. Antenna Geometry.

The antenna array was installed on a FR-4 substrate with the following specifications $\varepsilon_r = 4.4$, tan $\delta = 0.02$, and thickness of 1.6mm.

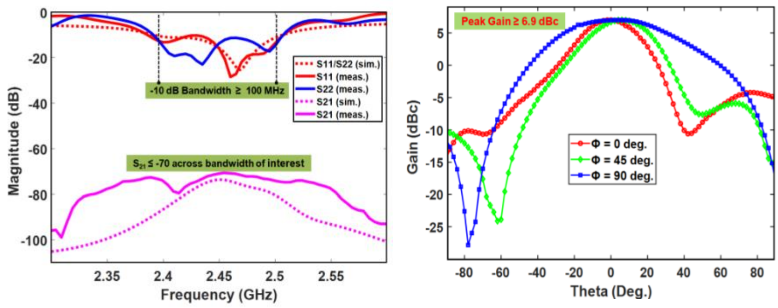

(a) (b)

Figure 31. S-parameter Plot (a) and Gain Plot (b) for Given Design.

The assembled antenna system offers better than 70 dB isolation levels over the whole matching bandwidth of 100 MHz. For T_x mode of antenna prototype offer better than 6.9 dBc peak gain.

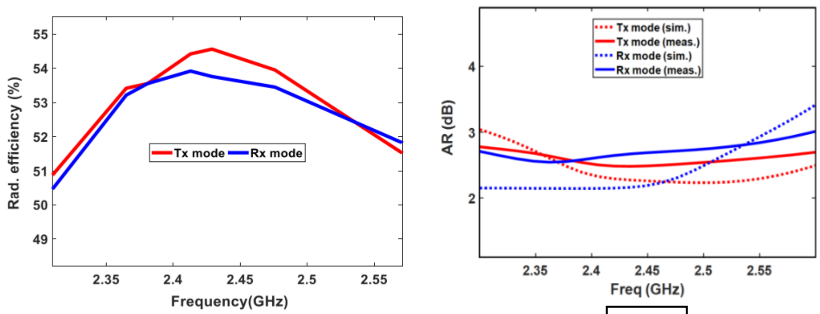

(c) (d)

Figure 32. (c) Radiation Efficiency plot (d) and Axial-Ratio Plot.

For both T_x and R_x modes, the measured radiation efficiency is superior than 53%. The given IBFD antenna validation model has a $|AR| \leq 3$dB over the whole matching bandwidth of 100 MHz (2.40 GHz to 2.50

GHz). These AR vs frequency data support the intended CP characteristics for the T_x and R_x ports' whole matching bandwidth of antenna.

4.4.10 Survey 10

This work describes the development of an improved isolation and gain multiple input multiple output (MIMO) antenna based on metamaterials. Above the MIMO antenna is a superstrate made of brand-new hexagonal nested loop double negative (DNG) metamaterial by absorbing the magnetic fields near field component, superstrate lowers the mutual coupling (MC) between the antenna elements.

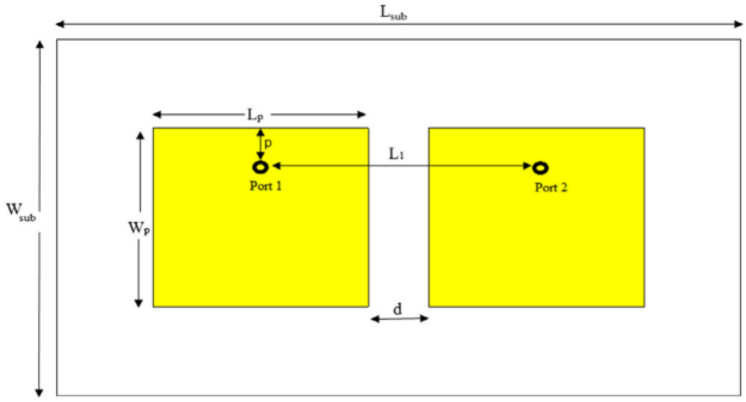

Figure 33. Top view of Antenna Geometry.

The measurements are as follows: L_{sub} = 60 mm, W_{sub} = 32 mm, H = 9 mm, L_p = 18 mm, W_p = 16 mm, L_1 = 22 mm, p = 4 mm, and d = 5 mm. The design is printed with ε_r= 2.33 on a 60× 32×1.57 mm3. RT/Duroid 5870 substrate with a 5 mm ($0.095\lambda_0$) edge-to-edge spacing. two patches for the optimum antenna performance.

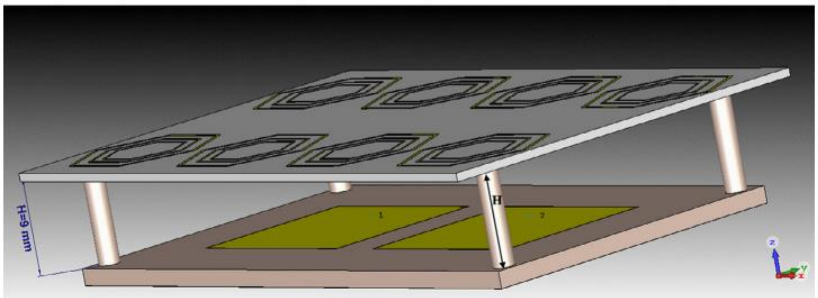

Figure 34. Side view of Antenna Geometry.

The superstrate structure utilized with this antenna is made up of 8-unit cells printed in 4x2 rows on top of a (60 × 40 mm2) substrate with no copper on the bottom side. The gap between the two rows of unit cells is 10 mm, and it is designed for improved isolation. Using a hollow plastic rod as support, the superstrate is held at a height H = 9 mm above the patch antenna to achieve isolation better than 24 dB in the 5.6 GHz to 6.05 GHz frequency band.

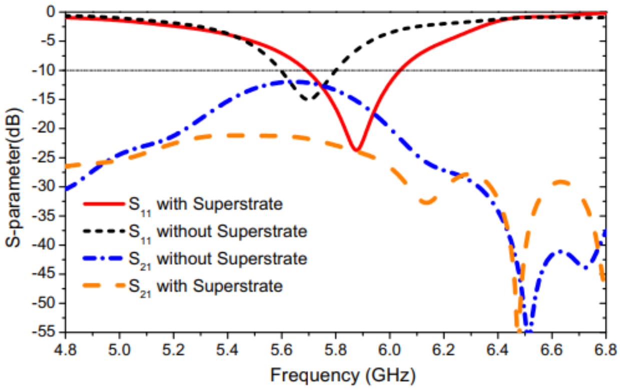

Figure 35. S parameter Plot for Given Design.

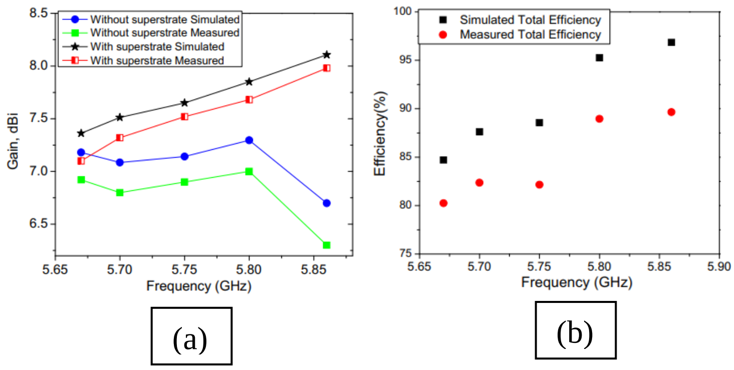

Figure 36. Gain Plot (a) and Efficiency Plot (b) for Given Design.

Antenna efficiency continues to be above 80%. Because of the structure of the metamaterial superstrate, the antenna's measured gain increased from 6.3 dBi to 7.98 dBi, or by 1.68 dBi, at the resonance frequency (5.7GHz).[11].

4.5 Summary of Literature Survey.

From the above literature review, it was analyzed that all the papers based on full-duplex systems were designed on the lower frequency band (2.4GHz, 5.9GHz) and a very few papers are available at mm-wave frequency band for full-duplex antenna system. Therefore, this study focusses on mm-wave frequency.

The SI cancellation methods described in the literature can be broadly split into two categories: passive and active, with analogue and digital procedures falling under the active category. In the FD system, the passive mode of SI cancellation, also referred to as "antenna cancellation," relies on the mutual coupling reduction of the transmitter and reception antennas, whereas the active SI reduction strategies are applied in the analog/digital base-band stages. However, prior to digital SI cancellation, analog SI cancellation is unable to offer enough isolation to prevent the saturation of active components such the analog-to-digital converter (ADC) and low nose amplifier (LNA). Use of passive antenna mutual coupling (MC) reduction techniques in FD antenna systems is therefore wise in order to supplement active (analog and digital) SI cancellation techniques and lower system cost.

4.6 Isolation techniques.

The most straightforward technique to create isolation between antennas is to increase their distance from one another, although doing so would make the structure larger. To reduce the mutual coupling between antennas, a variety of techniques have been developed. Several cancellation approaches have been published in the literature for reducing isolation at the antenna stage. Defective ground structures (DGS), Polarization Diversity, Electromagnetic Band Gaps (EBG), Beam Forming Networks, near field cancellation, Metamaterial-Based Superstrate, and 180° hybrid coupler is a few of these techniques.

4.6.1 Defected Ground Structure (DGS)

Surface waves that cause self-interference may be suppressed by DGS structures. Surface waves travel along the ground plane and are unwanted waves. These surface waves can be interfered with, hence lowering self-interference, by integrating DGS patterns or structures. To improve isolation even more, DGS can employ shielding and absorbent materials. Metal plates or conducting sheets can act as shielding materials to prevent electromagnetic fields and reduce coupling. By absorbing and dissipating undesired electromagnetic radiation, absorbing materials can reduce self-interference.

4.6.2 Polarization Diversity

Self-interference can be decreased by using antennas with different polarisation properties, such as one antenna with vertical polarisation and the other with horizontal polarisation. The coupling effects can be reduced by maintaining orthogonal polarisations between the transmitting and receiving antennas.

4.6.3 Electromagnetic Band Gaps (EBG)

Self-interference can be efficiently suppressed by using EBG structures to form a stopband or bandgap in the frequency spectrum. Periodic patterns or structures that demonstrate electromagnetic wave attenuation within the appropriate frequency range of self-interference are introduced by the EBG structures. This reduces the possibility of the transmitting signal interfering with the receive path. The isolation between the transmit and receive paths can be made better by adding EBG structures near the antenna elements or on the antenna substrate. By preventing electromagnetic wave leakage from the transmitting path to the receiving path, the EBG structures improve isolation while lowering self-interference.

4.6.4 Beam Forming Networks (BFN)

Beamforming is a signal processing technique that uses an array of antennas to steer the transmitted and received signals in specific directions. Beamforming networks are used in a full-duplex system to divide the transmit and receive paths into independent beams, permitting spatial separation and minimising self-interference.

4.6.5 Metamaterial-Based Superstrate

The term "metamaterial" refers to materials that have been designed artificially to have electromagnetic properties. They have characteristics like a low permittivity, a high permeability, and a negative refractive index that can be used to control how electromagnetic waves propagate. By suppressing the radiation in particular directions where self-interference occurs, the metamaterial superstrate can change the antennas' radiation characteristics. Energy coupling between antennas can be reduced and isolation can be improved by adjusting the superstrate's reflection and scattering properties.

4.6.6 180˚ hybrid coupler

A four-port device called a 180˚ hybrid coupler divides an input signal into two outputs of equal power and 180˚ phase differences. By combining two signals one in phase (0˚) and the other out of phase (180˚ it produces two orthogonal output signals that are orthogonal to one another. A 180˚ hybrid coupler can be used to divide the transmit and receive paths in a full-duplex antenna configuration. One of the hybrid coupler's output ports is connected to the broadcast path, and the other output port is connected to the receive path. The hybrid coupler's input port is connected to the shared antenna port. The two output ports of the hybrid coupler are designed to have high isolation, which means that the energy transmitted from the transmit path is minimized in the receive path, and vice versa.

4.6.7 Near Field Cancellation

A full-duplex system, transmits both far-field and near-field components in its broadcast signal from the transmit antenna. Self-interference can result from near-field components that propagate close to the antenna and strongly couple with the reception antenna. An antenna used to generate a signal that cancels out the near-field components of the transmitted signal is referred to as a near-field cancelling antenna, also known as an auxiliary or cancellation antenna. This cancellation signal is designed to have the same amplitude but an opposite phase to the near-field components, effectively nullifying their effect on the receive antenna.

Chapter 5

Single Band Full-Duplex Antenna at Millimeter Wave Frequency

5.1 Proposed Design 1

This work proposes a full-duplex microstrip patch antenna at 28 GHz (operating frequency) with strong T_x-R_x isolation which is based on a combination of isolation techniques i.e., a rectangular defective ground structure (DGS) slots (strip lines) and a metamaterial-based superstrate by absorbing the magnetic fields near field component. This design involves following steps to reach the final design.

Step-1

In this step we have designed a simple microstrip patch with copper cladding of 0.035mm is engraved on the top side of 0.3mm thick Roger (RO4003) substrate with relative permittivity (ε_r) of 3.55 and loss tangent of 0.0027 based on the initial calculation at millimeter wave frequency (i.e. 28GHz).

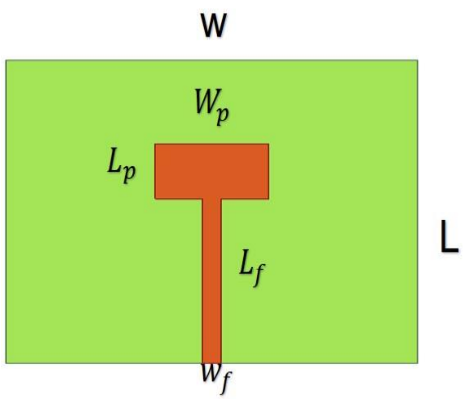

Figure 37. Top view of Microstrip Patch Antenna at 28 GHz.

Proposed microstrip patch antenna showing dimensions (in mm): Width of the Substrate (W) = 15, Length of the Substrate (L) = 15, Length of the Patch (L_p) = 2.72, Width of the Patch (W_p) = 3.55, Width of the Feed (W_f) = 0.67, Length of the Feed (L_f) = 1.6, Height of the Substrate (h) = 0.3.

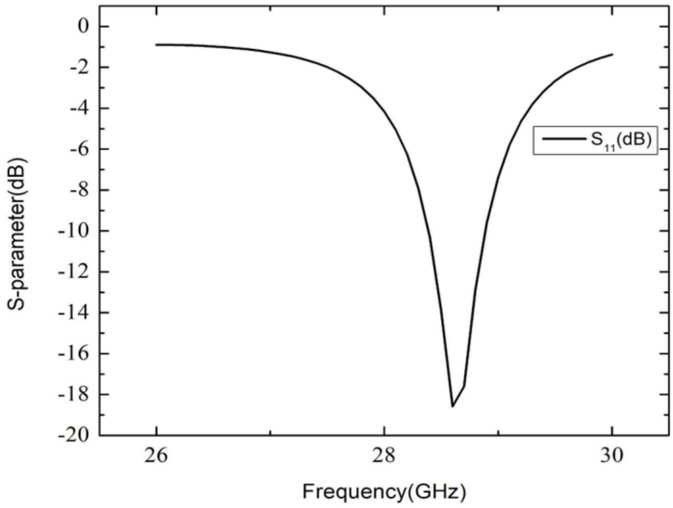

Figure 38. S-parameter Plot for given design at 28 GHz.

As a result, we observed that the impedance matching (S_{11}) is equal to -4.17 dB at 28 GHz (operating frequency) but at operating B.W (28.5 GHz to 28.75 GHz) is the impedance matching (S_{11}) is equal -18.57 dB.

Step-2

In order to get the impedance matching exactly at 28 GHz we have done parametric study by varying the patch dimension i.e. length of feed (L_f), width of feed (W_f), length of patch (L_p), width of patch (W_p) and we get the optimized value of the microstrip patch antenna at operating frequency.

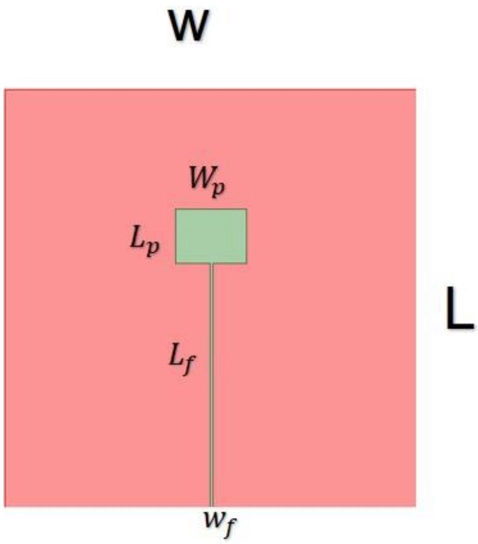

Figure 39. Top view of optimized Microstrip Patch Antenna at 28 GHz.

Optimized Microstrip Patch Antenna dimension (in mm): W =15, L=15, L_p=2.6, W_p=3.4, W_f=0.16, L_f=10, h=0.3.

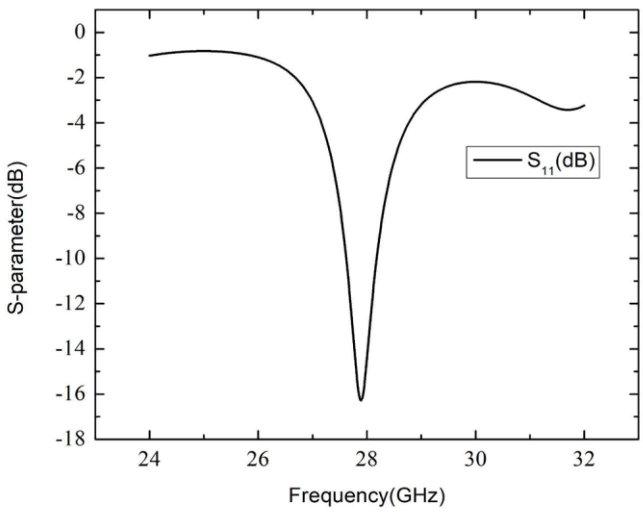

Figure 40. S-parameter of the Optimized Microstrip Patch Antenna at 28GHz.

We observe from the above graph that impedance matching (S_{11}) is equal to -17.29 dB, Gain is equal to 6.10dB, and Efficiency is 0.85 × 100 equals to 85 percent at 28GHz (operating frequency).

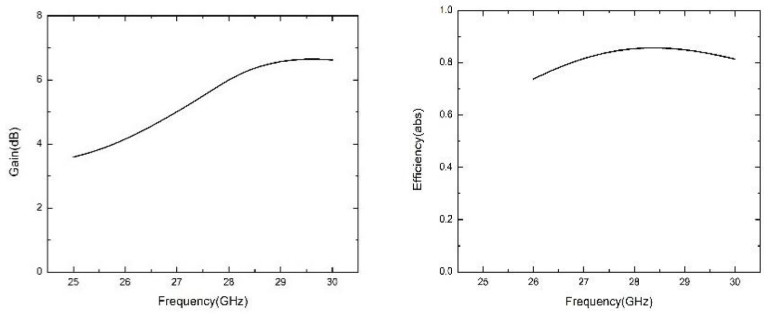

(a) (b)

Figure 41. Gain Plot (a) and Efficiency Plot (b) for Given Design.

Step-3

In this step, we design 2-port microstrip patch antenna are placed side-by-side configuration with $\lambda/2$ distance apart for full-duplex Trans-receiver system. This configuration was chosen in order to provide the best performance and the intended results, with the least amount of mutual coupling between the antennas.

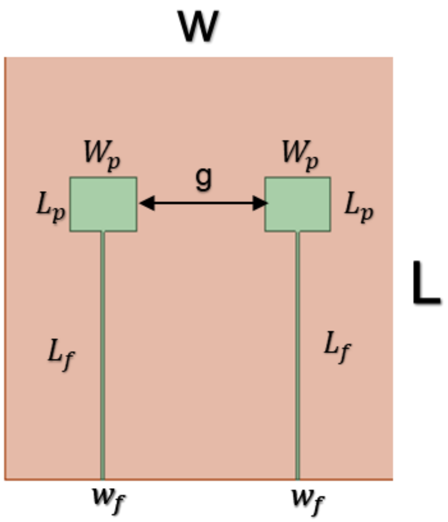

Figure 42. Top view of 2-Port Microstrip Patch Antenna at 28GHz.

2-Port Microstrip Patch Antenna dimension (in mm): W = 20, L = 20, L_p = 2.6, W_p = 3.4, W_f = 0.16, L_f = 10, h = 0.3, g = 5.35.

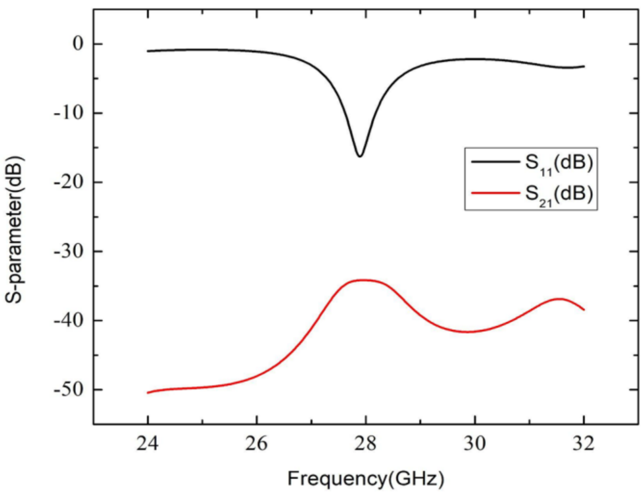

Figure 43. S-parameter of the 2-Port Microstrip Patch Antenna at 28 GHz.

Here, we observed that impedance matching (S_{11}) is equal to -14.42 dB and isolation or mutual coupling (S_{12}/S_{21}) between the antenna is -34.12 dB.

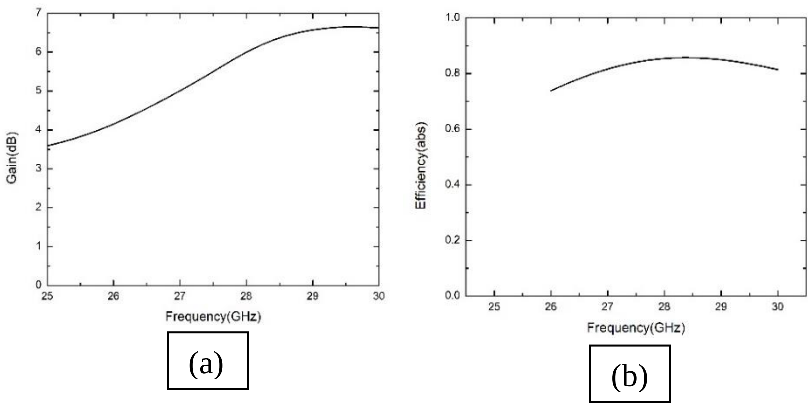

Figure 44. Gain Plot (a)Efficiency Plot (b) for Given Design.

The gain and efficiency from the above graph is equal to 6.1 dB and 85 percent at 28 GHz (operating frequency).

Step-4

Further, rectangular slots are drawn in the ground plane i.e known as Defected Structure Ground plane (DGS) to reduce self-interference or improve isolation by absorbing and dissipating undesired electromagnetic radiation.

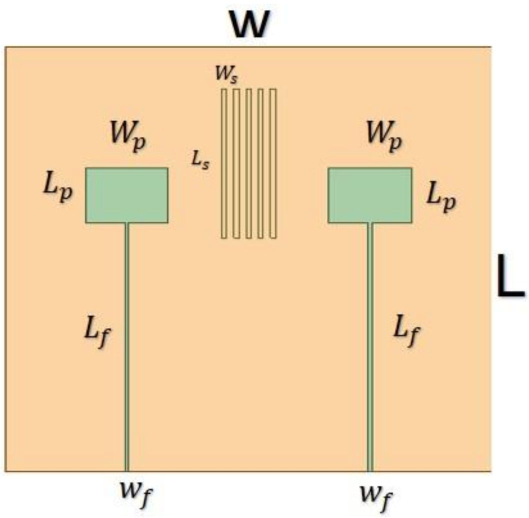

Figure 45. Top view of 2-Port Microstrip Patch Antenna with slots in the ground plane.

2-Port Microstrip Patch Antenna with slots in the ground plane dimension (in mm): W = 20, L = 20, L_p = 2.6, W_p = 3.4, W_f = 0.16, L_f = 10, h = 0.3, g = 5.35, l_s = 7.5 , w_s = 0.25, g_s = 0.1.

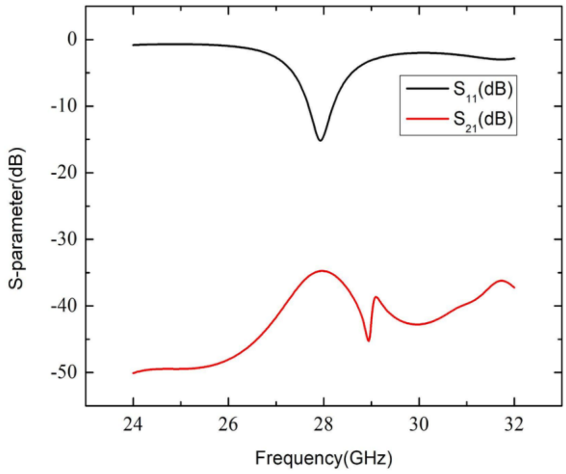

Figure 46. S-parameter of the 2-Port Microstrip Patch Antenna with slots in the ground plane.

Here, we observe that impedance matching (S_{11}) was equal to -14.45 dB and isolation or mutual coupling (S_{12}/S_{21}) between the antenna was improved from -34.12 dB to -45.27 dB.

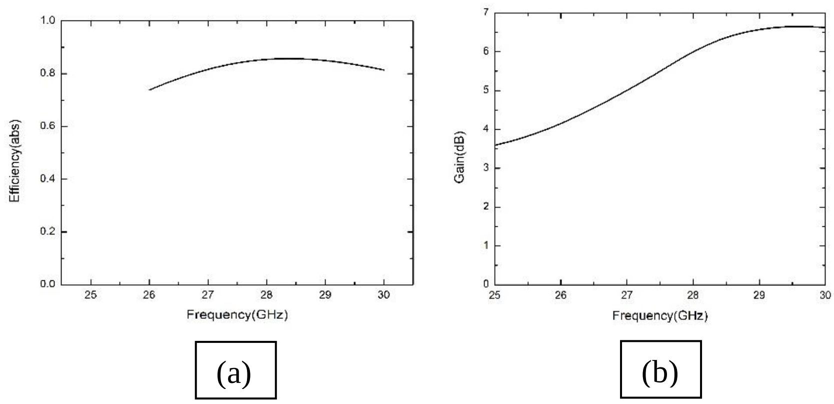

Figure 47. Gain Plot (a) and Efficiency plot (b) for Above Design.

It was observed that Gain of the above design was 6.04dB and efficiency was 0.88×100 equal to 88 percent.

Step-5

In the final step, the superstrate structure utilized with this antenna is made up of 8-unit cells printed in 27x2 rows on top of a (20 × 20 mm^2) substrate with no copper on the bottom side. The gap between the two rows of unit cells is 3.5mm, and it is designed for improved isolation. the superstrate is held at a height T_{su} = 3 mm above the patch antenna to enhanced isolation.

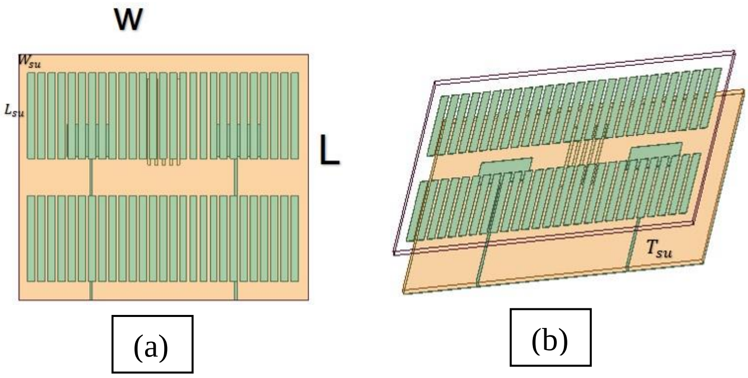

Figure 48. Top view (a) and Isometric View (b) of Proposed Antenna Geometry.

2-Port Microstrip Patch Antenna with metamaterial dimension (in mm): W = 20, L = 20, L_p = 2.6, W_p = 3.4, W_f = 0.16, L_f = 10, h = 0.3, g = 5.35, l_s = 7.5 , w_s = 0.25, g_s = 0.1, l_{su} = 6.5 , w_{su} = 0.5, T_{su} = 3.

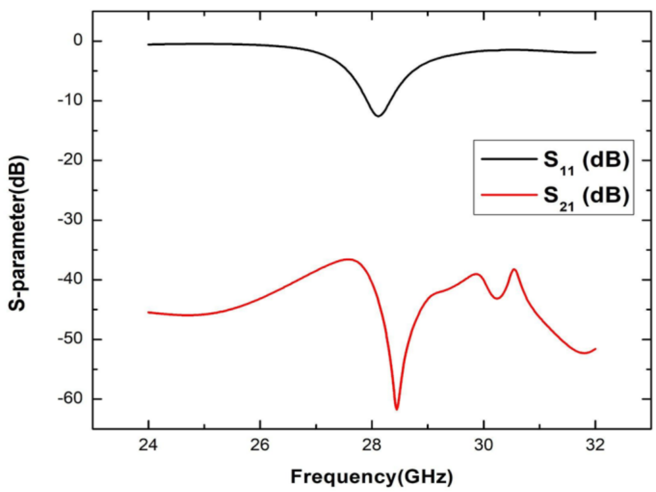

Figure 49. S-parameter of the Proposed Antenna.

From above S-parameter plot it can be seen that the resonance is achieved at 28GHz-28.4GHz over the frequency band with a value of -12.57dB and further isolation improved from -45.45dB to -61.50dB which is acceptable for full-duplex system.

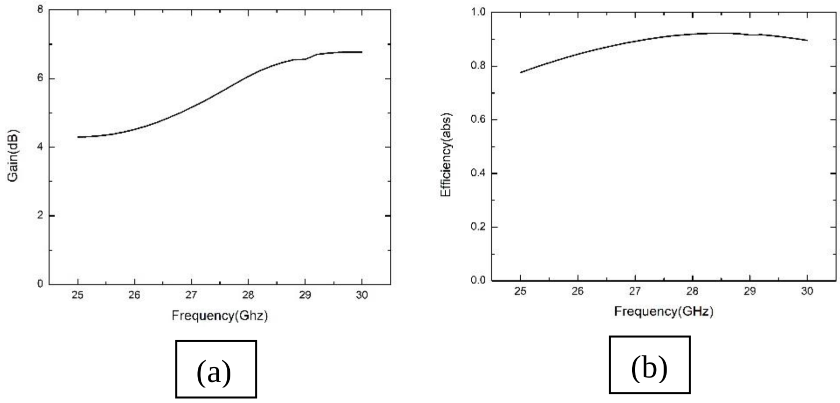

Figure 50. Gain Plot (a) and Efficiency plot (b) of the Proposed Antenna.

It was absorbed from the proposed design that the Gain and efficiency was 6dB and 0.91×100 is equal to 91 percent respectively.

5.2 Design 2

This work proposes a full-duplex microstrip patch antenna with another resonance frequency that is 38 GHz with high T_x-R_x isolation by adding a rectangular defective ground structure (DGS) slots (strip lines) in the ground plane of the configuration. This design involves following steps to reach the final design.

Step-1

In this step we have designed a simple microstrip patch with copper cladding of 0.035mm is engraved on the top side of 0.3mm thick Roger (RO4003) substrate with relative permittivity (ε_r) of 3.55 and loss tangent of 0.0027 based on the initial calculation at millimeter wave frequency (i.e. 38GHz).

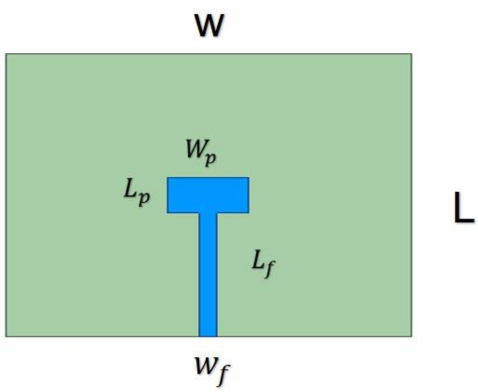

Figure 51. Top view of Microstrip Patch Antenna at 38 GHz.

Proposed microstrip patch antenna showing dimensions (in mm): Width of the Substrate (W) = 15, Length of the Substrate (L) = 15, Length of the Patch (L_p) = 1.91, Width of the Patch (W_p) = 2.69, Width of the Feed (W_f) = 0.67, Length of the Feed (L_f) = 1.19, Height of the Substrate (h) = 0.3.

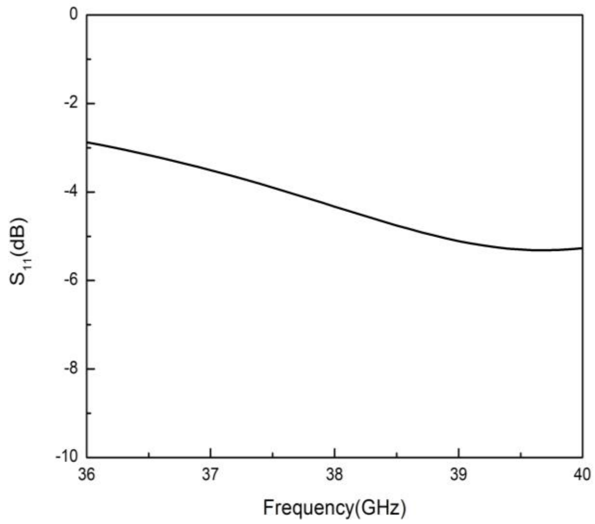

Figure 52. S-parameter of the Microstrip Patch Antenna at 38 GHz.

From the above, we observed that the impedance matching (S_{11}) is equal to -4.37 dB at 38 GHz (operating frequency).

Step-2

In order to get the impedance matching exactly at 28 GHz we are done parametric study by varying the patch dimension i.e. length of feed (L_f), width of feed (W_f), length of patch (L_p), width of patch (W_p) and we get optimized value of the antenna at operating frequency.

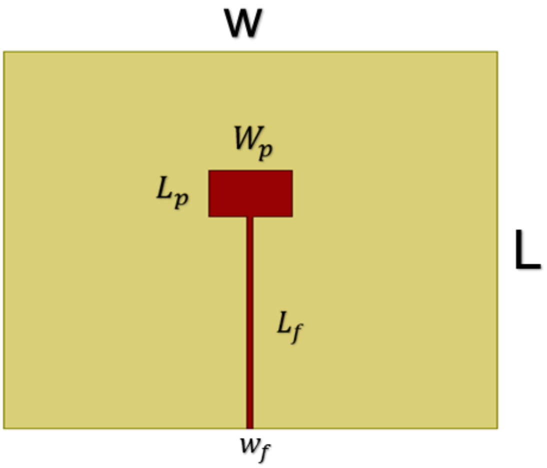

Figure 53. Top view of optimized Microstrip Patch Antenna at 38 GHz.

Optimized Patch dimension (in mm): W =15, L =15, L_p =1.85, W_p =2.49, W_f =0.18, L_f =10, h =0.3.

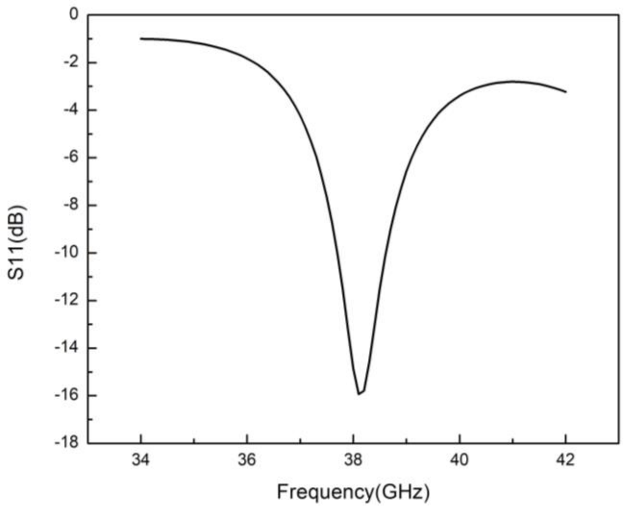

Figure 54. S-parameter of the Optimized Microstrip Patch Antenna at 38GHz.

The graph above shows that at 38GHz (the working frequency), impedance matching (S11) is equal to -14.97 dB.

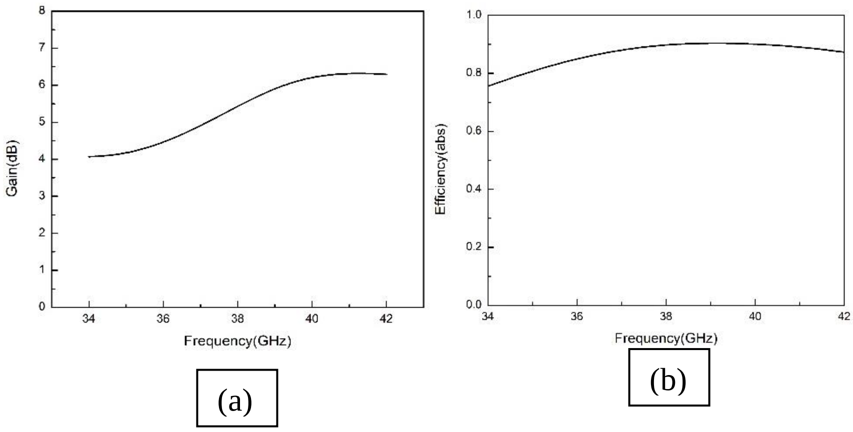

Figure 55. Gain Plot (a) and Efficiency Plot (b) for above design.

The gain and efficiency from the above graph is equal to 5.43 dB and 90 percent at 38 GHz (operating frequency).

Step-3

In this step, we have designed 2-port microstrip patch antenna are placed side-by-side configuration with $\lambda/2$ distance apart for full-duplex Trans- receiver system.

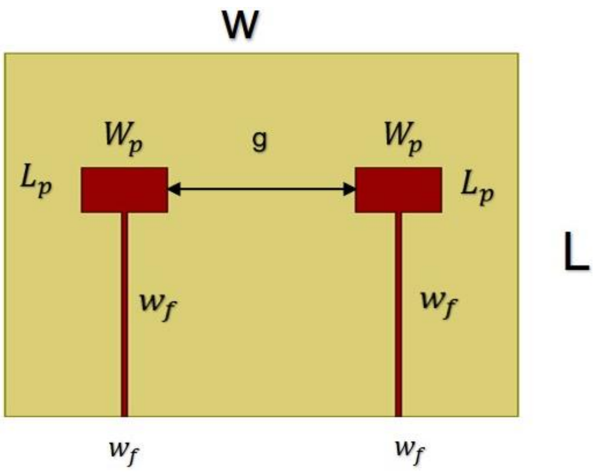

Figure 56. Top view of 2-Port Microstrip Patch Antenna at 38GHz (Side-by-Side Placement).

2-Port Patch dimension (in mm): W =15, L =15, L_p =1.85, W_p =2.49, W_f =0.18, L_f =10, h =0.3, g =4.

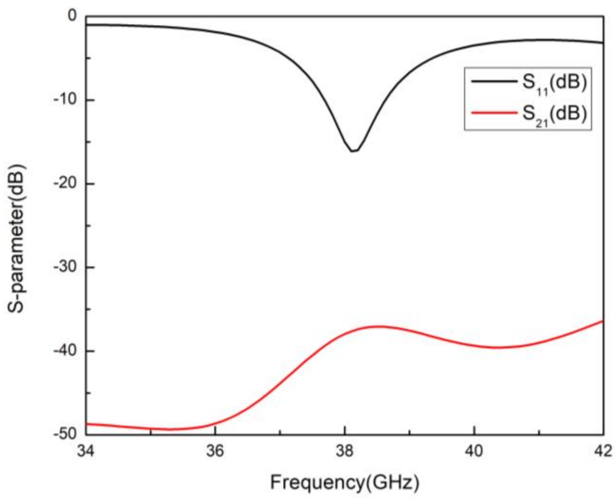

Figure 57. S-parameter of the 2-Port Microstrip Patch Antenna at 38 GHz (Side-by Side Placement).

Here, we observed that impedance matching (S_{11}) is equal to -15.15 dB and isolation or mutual coupling (S_{12}/S_{21}) between the antenna is -37.92 dB.

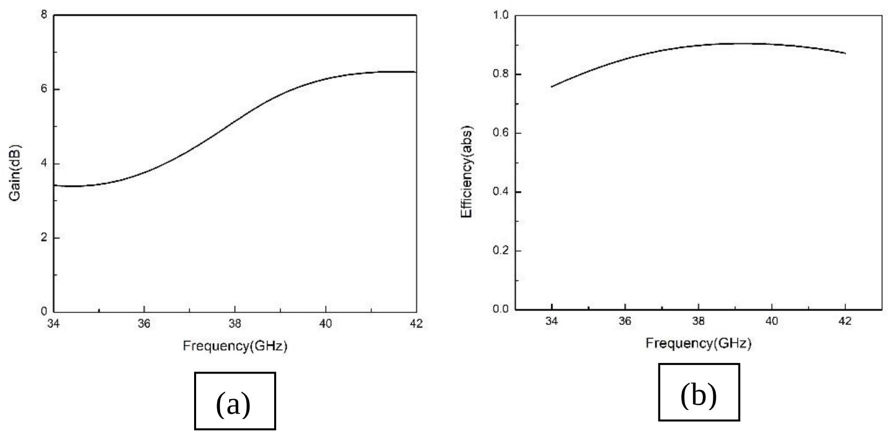

Figure 58. Gain Plot (a) and Efficiency Plot (b) for Given Design.

The gain and efficiency from the above graph is equal to 5.15 dB and 90 percent at 38 GHz (operating frequency).

Step-4

In this step, we design 2-port microstrip patch antenna are placed in orthogonal configuration which means both the antenna are orthogonal to other with $\lambda/2$ distance apart for full-duplex Trans- receiver system. This configuration was chosen in order to provide the best performance and the intended results, with the least amount of mutual coupling between the antennas.

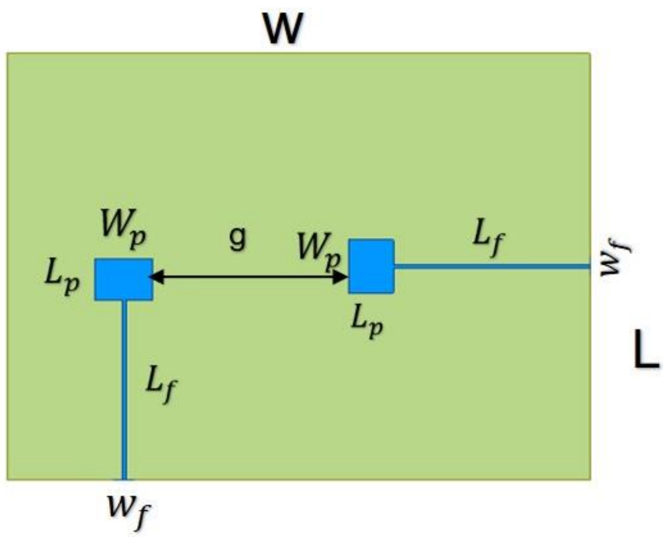

Figure 59. Top view of 2-Port Microstrip Patch Antenna at 38GHz (Orthogonal Placement).

2-Port Patch dimension (in mm): W =25, L =20, L_p =1.85, W_p =2.49, W_f =0.18, L_f =10, h =0.3, g =4.

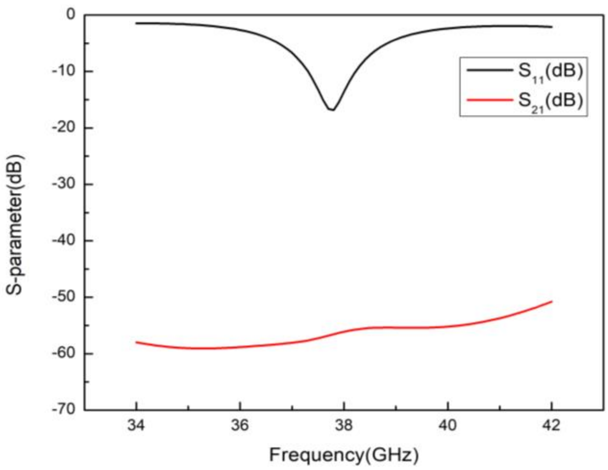

Figure 60. S-parameter of the 2-Port Microstrip Patch Antenna at 38 GHz (Orthogonal Placement).

The graph above shows that at 38GHz (the working frequency), impedance matching (S_{11}) is equal to -16.69 dB, isolation (S_{12}/S_{21}) is improved from -37.92 dB to -56.10 dB.

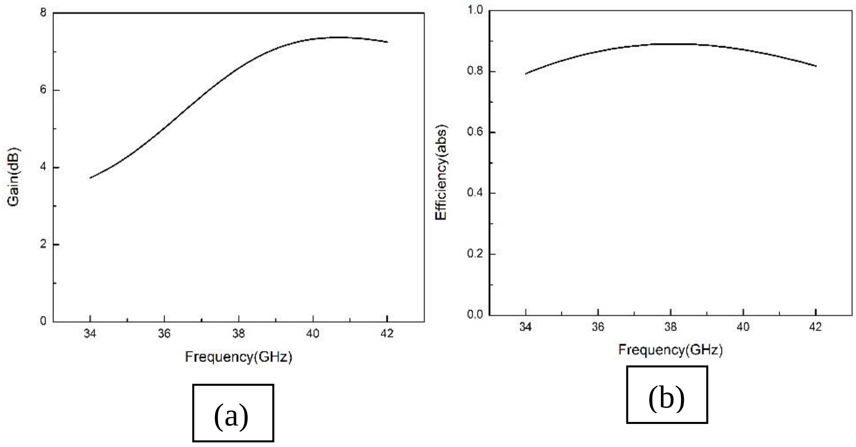

Figure 61. Gain Plot (a) and Efficiency Plot (b) for Given Design.

From the above graph, the Gain and Efficiency of the given antenna is equal to 6.58 dB, and 0.89×100, or 89%.

Step-5

Further, rectangular slots (strip lines) are drawn in the ground plane i.e known as Defected Structure Ground plane (DGS) to reduce self-interference or improve isolation by absorbing and dissipating undesired electromagnetic radiation.

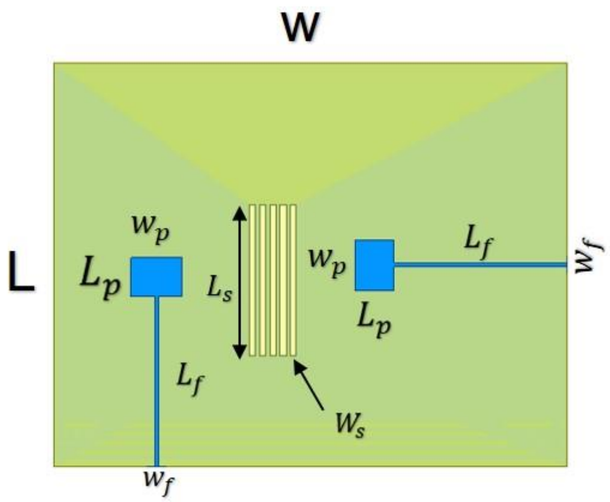

Figure 62. Top view of 2-Port Microstrip Patch Antenna at 38GHz with slots.

2-Port Microstrip Patch Antenna with slots in the ground plane dimension (in mm): W = 25, L = 20, L_p = 1.91, W_p = 2.49, W_f = 0.18, L_f = 10, h = 0.3, g = 4, l_s = 5.5 , w_s = 0.25, g_s = 0.2

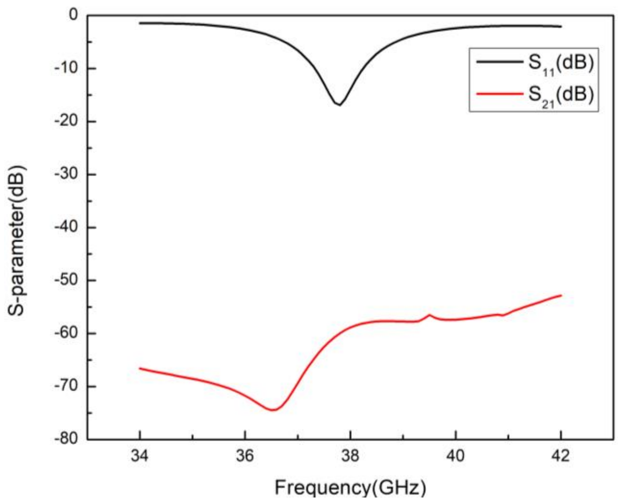

Figure 63. S-parameter of the 2-Port Microstrip Patch Antenna at 38 GHz with slots.

From above S-parameter plot it can be seen that the resonance is achieved at 37.79GHz-38GHz over the frequency band with a value of impedance matching (S_{11}) -16.89dB and further isolation (S_{12}/S_{21}) improved from -56.10B to -60.01dB which is acceptable for full-duplex system.

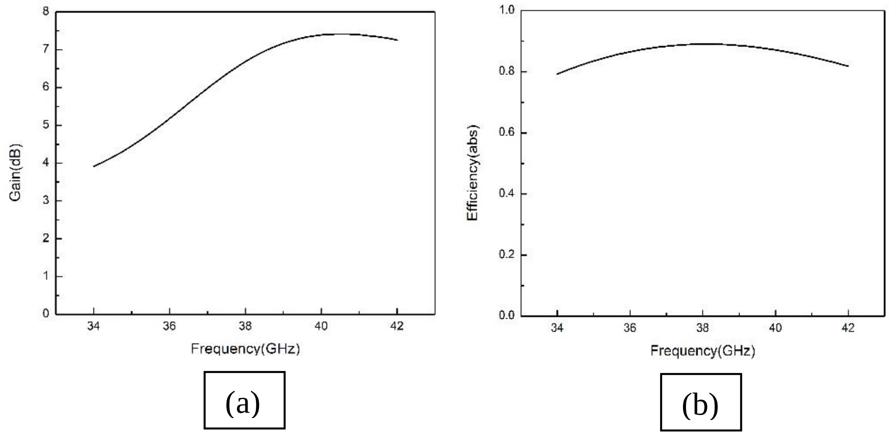

Figure 64. Gain Plot (a) and Efficiency Plot (b) for Given Design.

From the above graph, the Gain and Efficiency of the given antenna is equal to 6.59 dB, and 0.89×100, or 89%.

5.3 Design 3

In this design work we tried to reduce the size of the proposed antenna at 28 GHz for a full-duplex system. This design involves following steps to reach the final design.

Step-1

In this step we have designed a simple insert-fed microstrip patch with copper cladding of 0.035mm is engraved on the top side of 0.3mm thick Roger (RO4003) substrate with relative permittivity (ε_r) of 3.55 and loss tangent of 0.0027 based on the initial calculation at millimeter wave frequency (i.e. 28GHz).

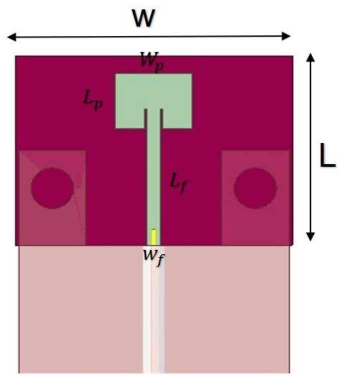

Figure 65. Top view of Reduced Microstrip Patch Antenna at 28 GHz (with connector).

Proposed microstrip patch antenna with reduced size showing dimensions (in mm): Width of the Substrate (W) = 13, Length of the

Substrate (L) = 9.3, Length of the Patch (L_p) = 2.7, Width of the Patch (W_p) = 3.6, Width of the Feed (W_f) = 0.67, Length of the Feed (L_f) = 8.6, Height of the Substrate (h) = 0.3, I_f = 1.

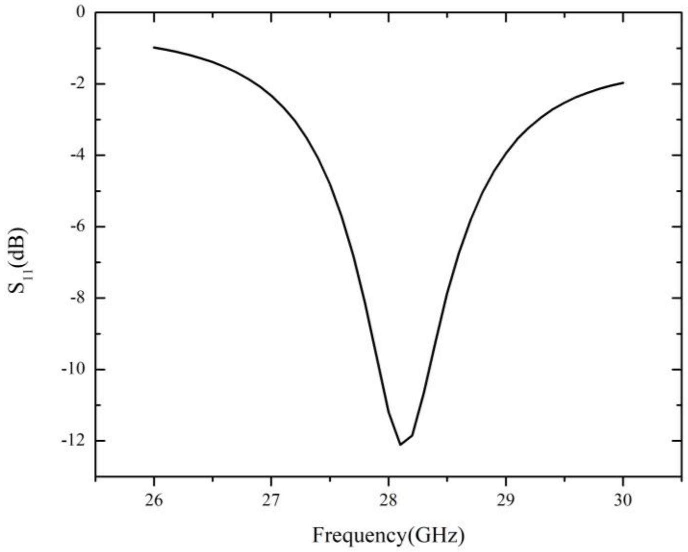

Figure 66. S-parameter of the Reduced Microstrip Patch Antenna.

As a result, we observed from the above S-parameter plot that the impedance matching (S_{11}) is equal to -12.07 dB at 28.11 GHz (operating frequency).

Step-2

In this step, we have designed 2-port microstrip patch antenna, placed orthogonal configuration with $\lambda/8$ distance apart for full-duplex Trans-receiver system to make design compact. This configuration was chosen in order to provide the best performance and the intended results, with the least amount of mutual coupling between the antennas.

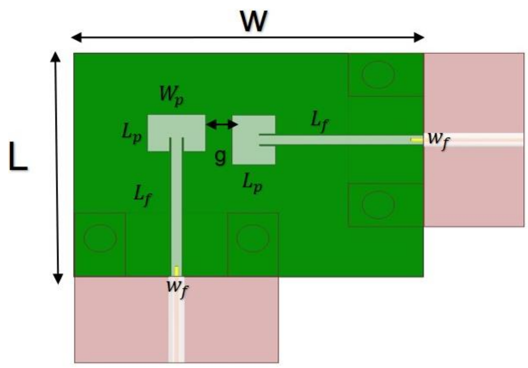

Figure 67. Top view of 2-Port Reduced Inset-Feed Microstrip Patch Antenna at 28 GHz.

2-Port Reduced Inset-Feed Microstrip Patch Antenna dimension (in mm): W =20.78, L=16.4, L_p =2.7, W_p =3.6, W_f =0.67, L_f =10, h =0.3, g = 1.33

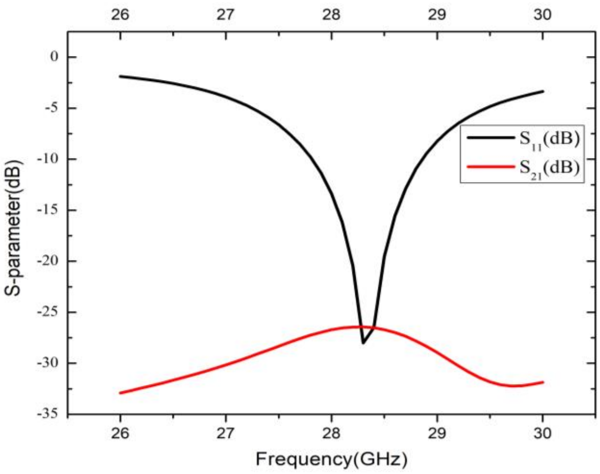

Figure 68. S-parameter of the 2-Port Inset- Feed Microstrip Patch Antenna at 28 GHz.

From the above S-parameter plot we observe that the impedance matching (S_{11}) is equal to -27.99 dB and isolation or mutual coupling (S_{12}/S_{21}) between the antenna is -26.44 dB at 28.11 GHz.

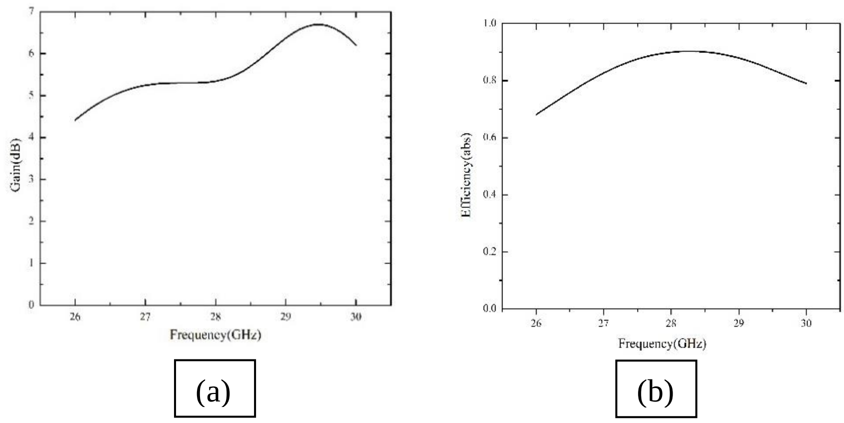

Figure 69. Gain Plot (a) and Efficiency Plot (b) for Given Design.

From the above graph, the Gain and Efficiency of the given antenna is equal to 5.72 dB, and 0.90×100, or 90%.

Step-4

Further, rectangular slots (3 strip line) are drawn in the ground plane between the two patches i.e known as Defected Structure Ground plane (DGS) to improve isolation by absorbing and dissipating undesired electromagnetic radiation.

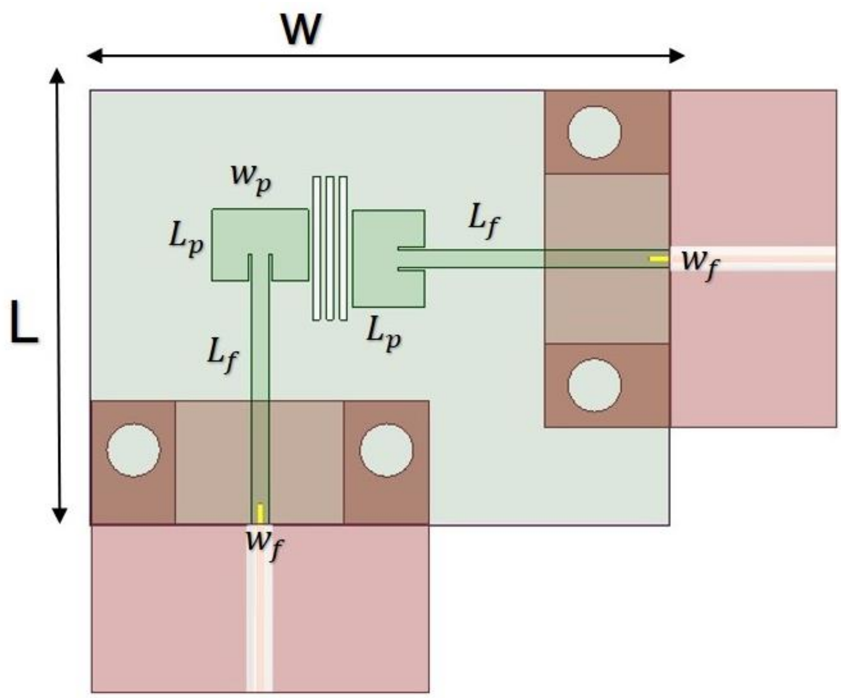

Figure 70. Top view of 2-Port Inset-Feed Microstrip Patch Antenna at 28GHz with slots.

2-Port Inset-Feed Microstrip Patch Antenna with slots in the ground plane dimension (in mm): W = 20.78, L = 16.4, L_p = 2.7, W_p = 3.6, W_f = 0.67, L_f = 10, h = 0.3, g = 1.33, l_s = 5.5 , w_s = 0.25, g_s = 0.2.

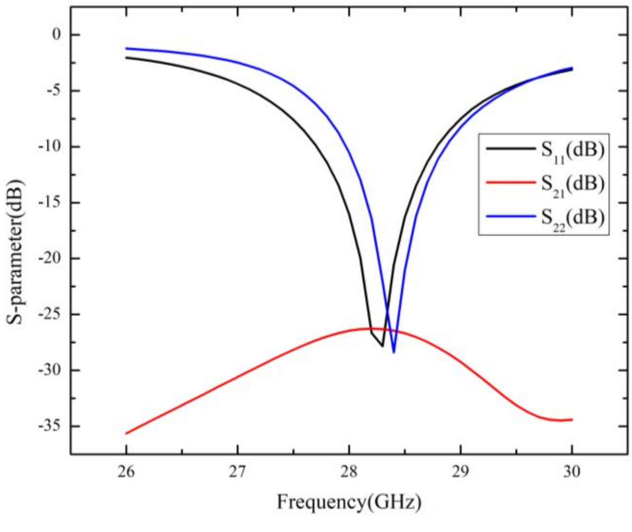

Figure 71. S-parameter of the 2-Port Inset- Feed Microstrip Patch Antenna at 28 GHz (with slots).

From the above S-parameter plot we observed that there is no improvement in the isolation or mutual coupling (S_{12}/S_{21}) between the antenna which is -26.30 dB at 28.21 GHz. Therefore, we further tried to reduce the self-interference by using another technique in the next step.

Step-5

In this phase, we put a number of metallic vias along the patch's width. The assumed via-diameter (d) and the space between the two subsequent vias (p) are 0.4mm and 0.6mm, respectively, which results in d/p = 0.66mm and limits the field-coupling between the radiating patches to improve the isolation.

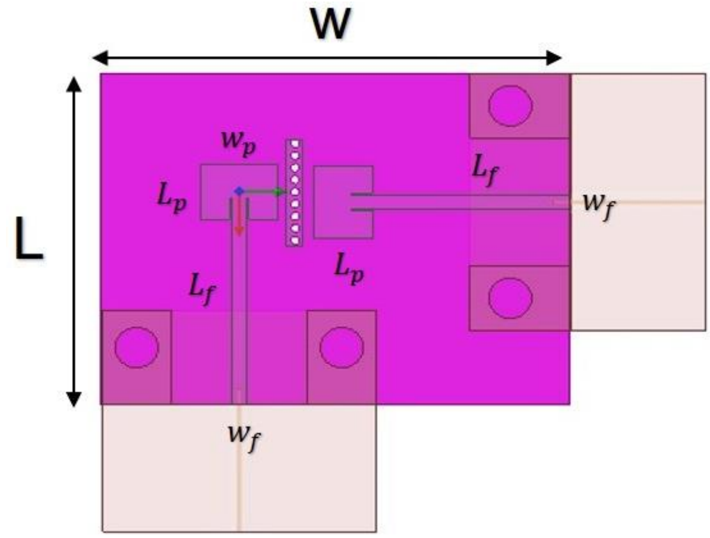

Figure 72. Top view of 2-Port Reduced Inset-Feed Microstrip Patch Antenna at 28 GHz (with metallic vias).

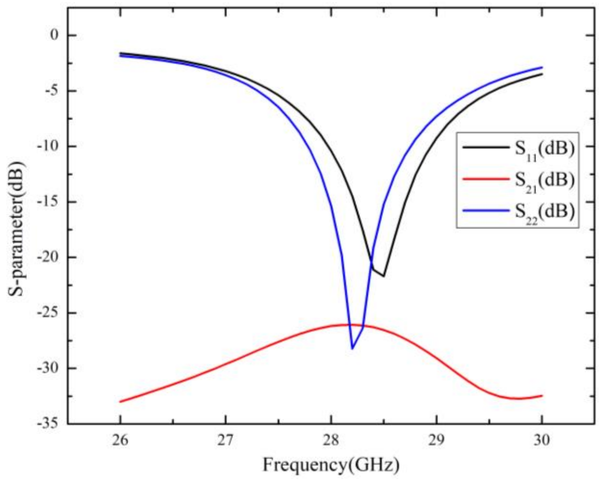

Figure 73. S-parameter of the 2-Port Inset- Feed Microstrip Patch Antenna at 28 GHz (with metallic vias).

From the above S-parameter plot we observed that there is no further improvement in the isolation or mutual coupling (S_{12}/S_{21}) between the antenna which is -26.07 dB at 28.20 GHz, therefore, we tried another configuration using this technique.

Step-5.1

In this case we placed the metallic vias along one of the radiating patch.

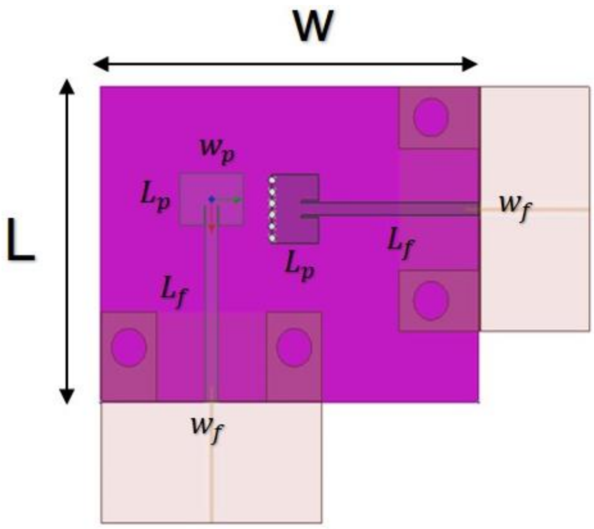

Figure 74. Top view of 2-Port Reduced Antenna at 28 GHz (with metallic vias).

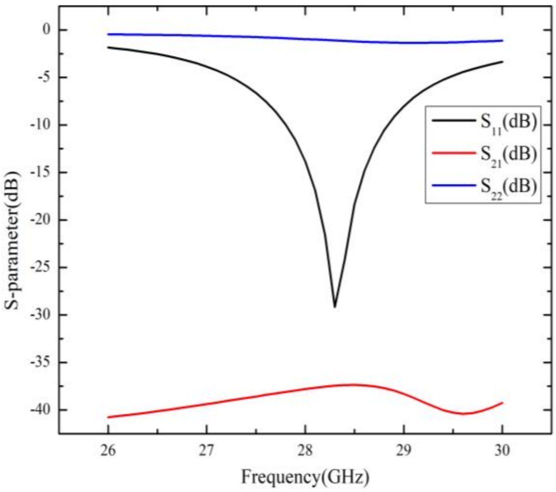

Figure 75. S-parameter of the 2-Port Inset- Feed Microstrip Patch Antenna at 28 GHz (with metallic vias).

From the above S-parameter plot we observed that there is improvement in the isolation (S_{12}/S_{21}) from -26.44 dB to 37.45 dB at 28.30 GHz but impedance matching (S_{11}) is equal to -1.11dB but it should be less than -10 Db which indicates that the antenna is not radiating properly. Hence, this technique does not work up to the mark.

5.4 Design 4

Step 1

In this work we tried to get a compact circularly polarized microstrip patch antenna for full-duplex system at 28 GHz. Therefore, we shifted the antennas with 30-degree angle in order to get reduced size and cp characteristics of antenna.

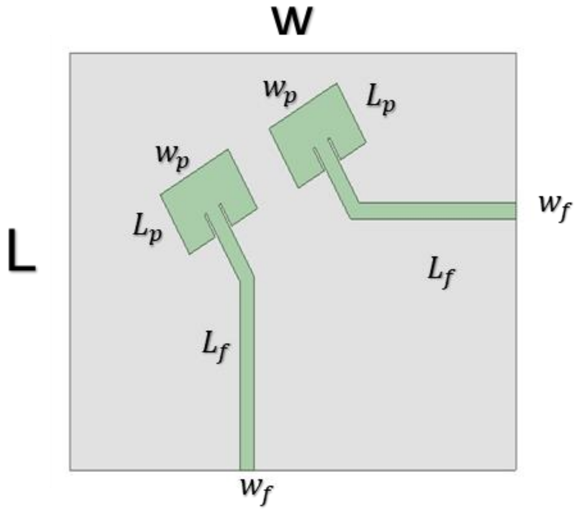

Figure 76. Top view of 2-Port Reduced Inset-Feed Microstrip Patch Antenna at 28 GHz with 30-degree shift.

2-Port Reduced Inset-Feed Microstrip Patch Antenna with 30-degree shift in the structure with dimension (in mm): W =20.78, L=16.4, L_p =2.7, W_p =3.6, W_f =0.67, L_f =10, h =0.3, g = 1.33.

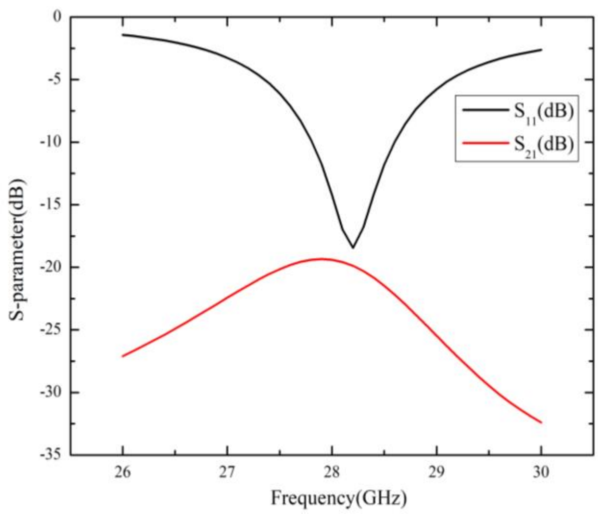

Figure 77. S-parameter of the 2-Port Inset- Feed Microstrip Patch Antenna at 28 GHz (with 30-degree shift).

From the above S-parameter plot we observed that there is further decrease in the isolation or mutual coupling (S_{12}/S_{21}) from -26.44 dB to -19.59 dB at 28.11 GHz, and impedance matching (S_{11}) is equal to -18.62 dB.

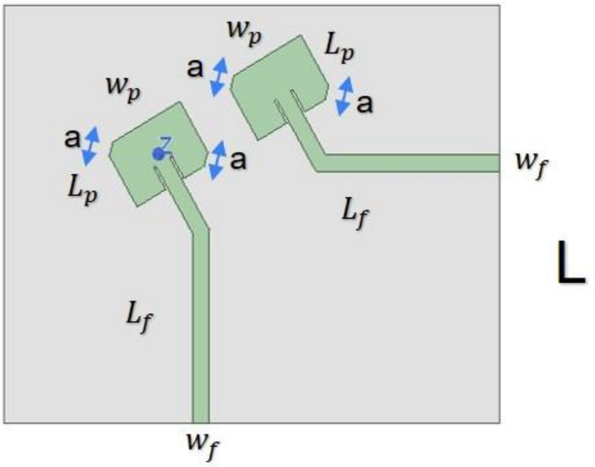

Figure 78. Top view of 2-Port Microstrip Antenna at 28 GHz with CP.

2-Port Reduced Inset-Feed Microstrip Patch Antenna with 30-degree shift in the structure with dimension (in mm): W =20.78, L=16.4, L_p =2.7, W_p =3.6, W_f =0.67, L_f =10, h =0.3, g = 1.33.

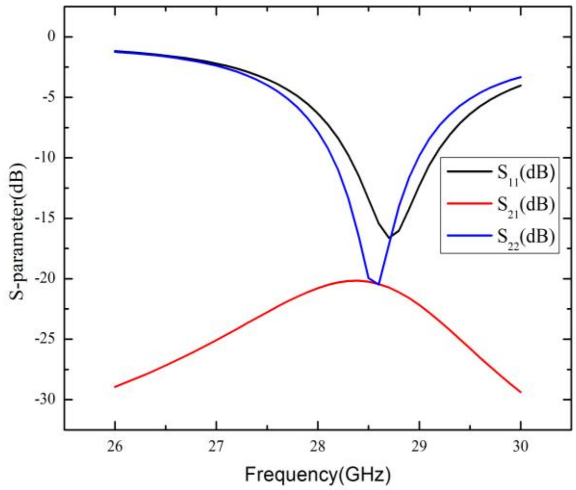

Figure 79. S-parameter of the 2-Port Inset- Feed Microstrip Patch Antenna at 28 GHz with CP.

From the above S-parameter plot we observed that there is further decrease in the isolation or mutual coupling (S_{12}/S_{21}) from -26.44 dB to -20.34 dB at 28.11 GHz as compared to the reduced 2-port microstrip antenna and impedance matching (S_{11}) is equal to -15.57 dB, (S_{22}) is equal to – 20.57dB.

Here, we can say that even though isolation has not improved much as expected but the antenna is designed with reduced size at 28GHz for full-duplex application.

Chapter 6

Conclusion and Future Work

Table1.

Comparison of the proposed two-port antenna with recent reported structure available in open literature.

References	Operating Frequency (GHz)	Isolation (dB)	Isolation technique and Feeding methods	Gain (dB)	Efficiency (%)
[2]	2.46	25	Line-feed with capacitive coupling	4	-
[3]	5.9	87	Field confinement, co-axial connector	5.63	-
[4]	5.85	90	Asymmetry+DGS+ NEDS, co-axial connector	7.11	97
[5]	2.4	36	Electric boundary using vias, inset-feed	-	-
[6]	5.6	60.8	Vias and stub Resonator, co-axial connector	6.65	-
[7]	2.4, 5.25 Dual-band	48,63	Orthogonal polarization +neutralization line +differential feeding	2.8, 6.3	-
[8]	2.40-2.52	30	Decoupling resonator, direct feeding	4.1	72
[9]	2.40	80	Pol. diversity + dif. feeding	6	75

[10]	2.4- 2.5	70	Near field cancellation,	6.9	50
[11]	5.68-6.05	24	Metamaterial superstrate, co-axial feeding.	7.98	85
Proposed Design 1.	28	61.50	DGS+ metamaterial superstrate, direct feeding	6	91
Design 2.	38	60	DGS, direct feeding	6.59	89

This thesis describes microstrip antenna configuration working on millimeter wave frequencies with good impedance matching (S_{11}) = -12.57 dB, and high inter-port isolation (S_{12}/S_{21}) = 61.50 dB, gain = 6 dB and efficiency of 91% whereas the impedance matching (S_{11}) = -16.89 dB, and high inter-port isolation (S_{12}/S_{21}) = 60.01 dB, gain = 6.59 dB and efficiency is 89% is presented for full-duplex application at (28-28.4 GHz) and (37.79-38 GHz) frequency band for 5G communication.

The relevant design steps are systematically described and S-parameter analysis were done. Table-1 clearly demonstrates that the performance is achieved in terms of high isolation without compromising much on the gain and efficiency. But while reducing the spacing between antenna (i.e. $\lambda/_8$) the performance were not good. Therefore, the proposed microstrip antenna system with $\lambda/_2$ spacing between antennas is an excellent candidate for full-duplex application, where self-interference cancellation through analog mode and isolation are desired attributes respectively.

Another analysis was done to introduced circularly polarized in the proposed antenna but we did not get optimal results, research is still going on.

6.1 Future Work.

Current work mainly concentrates on single band. In the future, full duplex antennas can work in multi-band applications. The isolation needs to be improved by adding some other techniques while keeping the antennas performance (gain, efficiency) constant. Current work focused on linearly polarized antennas and further extended to circularly polarized antennas. Besides this the Full-Duplex antenna proposed can be used as a suitable condition for 5G communication.

REFERENCES

[1] C. A. Balanis, Antenna theory: analysis and design, Fourth edition. Hoboken, New Jersey: Wiley, 2016.

[2] K. Kumari, M. Saikia, R. K. Jaiswal, S. Malik, and K. V. Srivastava, “A Compact, Low-Profile Shorted TM$_ {1/2,0}$ Mode Planar Co-polarized Microstrip Antenna for Full-Duplex Systems,” Antennas Wirel. Propag. Lett., vol. 21, no. 9, pp. 1887–1891, Sep. 2022.

[3] J. C. Dash and D. Sarkar, “A Co-Linearly Polarized Full-Duplex Antenna with Extremely High Tx-Rx Isolation,” Antennas Wirel. Propag. Lett., pp. 1–5, 2022.

[4] J. C. Dash and D. Sarkar, “Microstrip Patch Antenna System with Enhanced Inter-Port Isolation for Full-Duplex/MIMO Applications,” IEEE Access, vol. 9, pp. 156222–156228, 2021.

[5] Laller, Rupa, Mahesh P. Abegaonkar, and Ananjan Basu. "In-band Full-duplex Bistatic Antenna with reduced Mutual Coupling." 2022 IEEE Microwaves, Antennas, and Propagation Conference (MAPCON). IEEE, 2022.

[6] Dash, Jogesh Chandra, and Debdeep Sarkar. "A Co-Linearly Polarized Shared Radiator Based Full-duplex Antenna with High Tx-Rx Isolation using Vias and Stub Resonator." IEEE Transactions on Circuits and Systems II: Express Briefs (2023).

[7] Kumari K, Jaiswal RK, Srivastava KV. An in-band full-duplex antenna for dual-band application. Microw Opt Technol Lett. 2022;64:130–136.

[8] He, Yijing, and Yue Li. "Compact co-linearly polarized microstrip antenna with fence-strip resonator loading for in-band full-duplex systems." IEEE Transactions on Antennas and Propagation 69.11 (2021): 7125-7133.

[9] Nawaz, Haq, Noman Ahmad, and Javaria Aslam. "A unidirectional, printed antenna with high interport isolation over wider bandwidth for 2.4 GHz full duplex applications." IEEE Transactions on Antennas and Propagation 69.11 (2021): 7183-7191.

[10] Nawaz, Haq, et al. "Co-circularly polarized planar antenna with highly decoupled ports for S-Band full duplex applications." IEEE Access 10 (2022): 16101-16110.

[11] Mark, R., Rajak, N., Mandal, K. and Das, S., 2019. Metamaterial based superstrate towards the isolation and gain enhancement of MIMO antenna for WLAN application. AEU-International Journal of Electronics and Communications, 100, pp.144-152.

[12] Kumawat, P. and Joshi, S., 2020. Design of 28/38 GHz Dual-Band SIW Slot antenna for 5G Applications. *International Journal of Engineering Research and Technology (IJERT) ICEECT*, *8*(17).

[13] Niu, Bingjian, and Jie-Hong Tan. "Compact two-element MIMO antenna based on half-mode SIW cavity with high isolation." Progress In Electromagnetics Research Letters 85 (2019): 145-149.

[14] Zhang, Weiquan, et al. "Design of a stacked co-polarized full-duplex antenna with broadside radiation." IEEE Transactions on Antennas and Propagation 69.11 (2021): 7111-7118.

[15] Wu, Di, et al. "A compact, monostatic, co-circularly polarized simultaneous transmit and receive (STAR) antenna with high isolation." IEEE Antennas and Wireless Propagation Letters 19.7 (2020): 1127-1131.

[16] Li, Qianyi, and Ting-Yen Shih. "Characteristic-mode-based design of planar in-band full-duplex antennas." IEEE Open Journal of Antennas and Propagation 1 (2020): 329-338.

[17] Kumar, Praveen, Tanweer Ali, and MM Manohara Pai. "Electromagnetic metamaterials: A new paradigm of antenna design." IEEE Access 9 (2021): 18722-18751.

[18] Tu, Duong Thi Thanh, et al. "Improving Characteristics of 28/38GHz MIMO Antenna for 5G Applications by Using Double-Side EBG Structure." J. Commun. 14.1 (2019): 1-8.

[19] Gemeda, Mulugeta & Fante, Kinde & Goshu, Hana & Goshu, Ayane. (2021). Design and Analysis of a 28 GHz Microstrip Patch Antenna for 5G Communication Systems. VOLUME 8. 881-886.

[20] Lai, F.P., Chang, L.W. and Chen, Y.S., 2020. Miniature dual-band substrate integrated waveguide slotted antenna array for millimeter-wave 5G applications. *International Journal of Antennas and Propagation*, *2020.*